



Bzdek, B., & Reid, J. (2017). Aerosol microphysics: from molecules to the chemical physics of aerosols. *Journal of Chemical Physics*, 147(22), [220901]. <https://doi.org/10.1063/1.5002641>

Publisher's PDF, also known as Version of record

License (if available):
CC BY

Link to published version (if available):
[10.1063/1.5002641](https://doi.org/10.1063/1.5002641)

[Link to publication record in Explore Bristol Research](#)
PDF-document

This is the final published version of the article (version of record). It first appeared online via AIP at <https://aip.scitation.org/doi/abs/10.1063/1.5002641> . Please refer to any applicable terms of use of the publisher.

University of Bristol - Explore Bristol Research

General rights

This document is made available in accordance with publisher policies. Please cite only the published version using the reference above. Full terms of use are available:
<http://www.bristol.ac.uk/pure/about/ebr-terms>

Perspective: Aerosol microphysics: From molecules to the chemical physics of aerosols

Bryan R. Bzdek, and Jonathan P. Reid

Citation: *The Journal of Chemical Physics* **147**, 220901 (2017); doi: 10.1063/1.5002641

View online: <https://doi.org/10.1063/1.5002641>

View Table of Contents: <http://aip.scitation.org/toc/jcp/147/22>

Published by the [American Institute of Physics](#)

Articles you may be interested in

[Perspective: Highly stable vapor-deposited glasses](#)

The Journal of Chemical Physics **147**, 210901 (2017); 10.1063/1.5006265

[Editorial: JCP Communications—Updating a valued community resource](#)

The Journal of Chemical Physics **148**, 010401 (2018); 10.1063/1.5019731

[Perspective: Theory of quantum transport in molecular junctions](#)

The Journal of Chemical Physics **148**, 030901 (2018); 10.1063/1.5003306

[Communication: The \$\text{Al} + \text{CO}_2 \rightarrow \text{AlO} + \text{CO}\$ reaction: Experiment vs. theory](#)

The Journal of Chemical Physics **147**, 171101 (2017); 10.1063/1.5007874

[Communication: Symmetry-adapted perturbation theory with intermolecular induction and dispersion energies from the Bethe–Salpeter equation](#)

The Journal of Chemical Physics **147**, 181101 (2017); 10.1063/1.5007929

[Perspective: Surface freezing in water: A nexus of experiments and simulations](#)

The Journal of Chemical Physics **147**, 060901 (2017); 10.1063/1.4985879

PHYSICS TODAY

WHITEPAPERS

ADVANCED LIGHT CURE ADHESIVES

Take a closer look at what these environmentally friendly adhesive systems can do

READ NOW

PRESENTED BY
 MASTERBOND
ADHESIVES | SEALANTS | COATINGS

Perspective: Aerosol microphysics: From molecules to the chemical physics of aerosols

Bryan R. Bzdek^{a)} and Jonathan P. Reid^{a)}

School of Chemistry, University of Bristol, Bristol BS8 ITS, United Kingdom

(Received 31 August 2017; accepted 7 November 2017; published online 8 December 2017)

Aerosols are found in a wide diversity of contexts and applications, including the atmosphere, pharmaceuticals, and industry. Aerosols are dispersions of particles in a gas, and the coupling of the two phases results in highly dynamic systems where chemical and physical properties like size, composition, phase, and refractive index change rapidly in response to environmental perturbations. Aerosol particles span a wide range of sizes from 1 nm to tens of micrometres or from small molecular clusters that may more closely resemble gas phase molecules to large particles that can have similar qualities to bulk materials. However, even large particles with finite volumes exhibit distinct properties from the bulk condensed phase, due in part to their higher surface-to-volume ratio and their ability to easily access supersaturated solute states inaccessible in the bulk. Aerosols represent a major challenge for study because of the facile coupling between the particle and gas, the small amounts of sample available for analysis, and the sheer breadth of operative processes. Time scales of aerosol processes can be as short as nanoseconds or as long as years. Despite their very different impacts and applications, fundamental chemical physics processes serve as a common theme that underpins our understanding of aerosols. This perspective article discusses challenges in the study of aerosols and highlights recent chemical physics advancements that have enabled improved understanding of these complex systems. © 2017 Author(s). All article content, except where otherwise noted, is licensed under a Creative Commons Attribution (CC BY) license (<http://creativecommons.org/licenses/by/4.0/>). <https://doi.org/10.1063/1.5002641>

I. INTRODUCTION

Aerosols are dispersions of liquid droplets and/or solid particles in the gas phase that have wide ranging industrial applications as well as environmental and health impacts. For example, aerosols in the workplace or atmosphere can deleteriously impact health,^{1,2} but aerosols can also be efficient delivery agents of pharmaceuticals.³ Atmospheric aerosols predominantly scatter solar radiation, helping to offset warming due to greenhouse gases, though the magnitude of this effect remains relatively poorly constrained.⁴ Industrial aerosol applications include inkjet printing and spray drying.⁵ Despite the wide range of aerosol processes and impacts, the fundamental processes underpinning our understanding of aerosols in this broad range of contexts are similar. For example, many of the processes that govern the atmospheric lifetimes and concentrations of aerosols, such as condensational growth, chemical reaction, and coalescence, are also central to understanding aerosols upon inhalation to the respiratory tract, in personal care products, and in nano- and micro-particle fabrication using approaches like spray drying. Conventional analytical tools provide a snap shot of particle properties, reporting particle size distributions, mass concentrations, and chemical composition at a particular moment in time.⁶ However, the intimate coupling of gas and

particle phase composition through interfacial transport leads to dynamic changes in particle size, composition, and phase on time scales spanning from microseconds to days.⁷ A fuller understanding of aerosol properties and the refinement of predictive tools can only result if these dynamic processes are completely understood and accounted for, requiring measurements and models that address the relevant time scales and lengthscales.

Starting from the microphysical world of the single particle, recent developments in experimental and modeling capabilities are now yielding mechanistic insights that provide a level of resolvable detail that was previously inaccessible. Many of these developments have arisen from work at the forefront of chemical physics and physical chemistry (see Refs. 8–13 for a very small subset of examples). Without attempting to provide an exhaustive account, we highlight some of these developments and identify some of the emerging challenges, providing a perspective on aerosol research from the viewpoint of chemical physics. In this discussion, we progress from considering the processes operative at the molecular level during particle formation and growth through to the role of molecular processes at the particle interface in governing collective aerosol properties and then to the complex processes that occur in the particle bulk. This progression, along with some of the key chemical physics challenges associated with each stage, is illustrated in Fig. 1. We first define the time scales and lengthscales relevant to understanding aerosol dynamics.

^{a)}Authors to whom correspondence should be addressed: b.bzdek@bristol.ac.uk and j.p.reid@bristol.ac.uk.

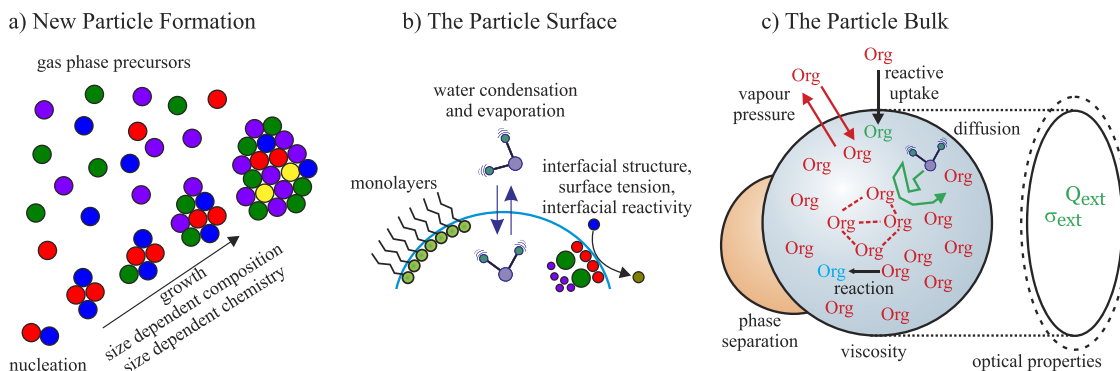


FIG. 1. Pictorial description of some of the chemical physics challenges associated with (a) particle formation and growth, (b) the particle surface, and (c) the particle bulk.

II. DEFINITION OF THE PROBLEM

It is first appropriate to identify the limits of this review. We will focus almost exclusively on understanding aerosol microphysics and chemistry, rather than the collective properties of the aerosol ensemble (i.e., across a particle population) and the role of fluid dynamics in transporting mass and heat in, for example, dense sprays and turbulent flows. With this in mind, the perspective we will take will centre on the processes occurring on an individual particle and extend only to the dynamics occurring when two particles encounter and coalesce. Aerosol processes can be probed from either the perspective of the condensed particle phase or the perspective of the gas phase. However, to fully characterise aerosols, both the condensed particle and the gas phases must be characterised.

As the core to any problem in chemical physics, we must begin by considering the molecular scale. At atmospheric pressure (1 atm) and temperature, simple considerations from gas kinetic theory indicate that there is 1 molecular collision with a 10 \AA^2 area at a particle surface in 10 ns. Similarly, the estimated residence time scale for a molecule at the surface of a liquid is ~ 1 ns. These values establish the lower limits of time scale and lengthscale that must be considered when exploring the dynamics of aerosols. Although potentially optimistic, it is imperative that any rigorous understanding of aerosol dynamics start here. Collectively, molecular properties establish the behaviour of nucleating clusters, the non-ideal interactions in complex mixtures that determine thermodynamic properties such as vapour pressure, and the flux of mass and heat that governs exchange between the phases. Thus, even in addressing problems as complex as the distribution of the semi-volatile material between the condensed and gas phases in aerosols and the resulting mass concentrations of aerosol particles in polluted urban environments, quantifying molecular properties as fundamental as vapour pressures is critical.¹⁴

Building up in scale from molecules, the interactions and collective properties of molecular clusters are key to understanding new particle formation and are sometimes amenable to experiment and quantum chemistry.^{15–18} Clearly, typical bulk phase properties such as surface tension have ambiguous meaning when considered for clusters consisting of only a few molecules. The growth of these

clusters, once beyond a critical radius, must still be inherently considered a molecular process.^{19–23} For particle sizes much smaller than the mean free path between collisions for gas phase molecules, the gas phase cannot be conceived as being continuous but is instead discrete in nature. Condensation rates (considered as a molar flux, J) can be accurately calculated from the Hertz-Knudsen equation (a gas kinetics approach), determining growth rates from collision frequencies and collision cross sections.^{24,25} Indeed, from a molecular perspective, it is not beyond doubt that every collision between a gas phase molecule and the growing particle surface leads to accommodation.²⁵ Only a fraction of molecular collisions may lead to the formation of favourable intermolecular interactions at the surface while dissipating the collision energy sufficiently rapidly for accommodation to be achieved.²⁶ This parameter is frequently recognised by establishing the probability for mass accommodation, α_M , which is the fraction of molecules colliding with a surface that are accommodated in the particle bulk. Notably, exquisite molecular beam experiments²⁷ and molecular dynamics simulations²⁸ can be used to probe the molecular nature of this interfacial exchange.

As the particle size increases relative to the mean free path, often quantified by the change in the Knudsen number (Kn, the ratio of the mean free path to droplet diameter), the gas phase becomes more continuous in nature and can be considered as a fluid without identifying discrete molecular units. Then, processes such as condensation can be considered to result from diffusion along a concentration gradient in the gas phase, and condensation fluxes can be calculated using the classic approaches first considered by Kelvin for evaporative/condensational fluxes of the bulk phase [Fig. 2(a)].⁷ The transition between these regimes typically occurs at a particle radius of ~ 200 nm at atmospheric pressure and temperature [Fig. 2(a)]. Reconciling these two limiting frameworks (often referred to as the *free molecule* and *continuum* regimes) into a unified treatment throughout the transition regime has been the focus of much discussion.^{24–26,29,30} As examples, cloud droplets and coarse mode aerosol particles larger than a few micrometres in radius in the atmosphere can be considered to fall within the continuum regime [Kn $\ll 1$, Fig. 2(b)], and evaporation/condensation fluxes and time scales are calculated by continuum theories. Small aerosol particles in the accumulation mode (particles $< 1 \mu\text{m}$ diameter) fall within the free

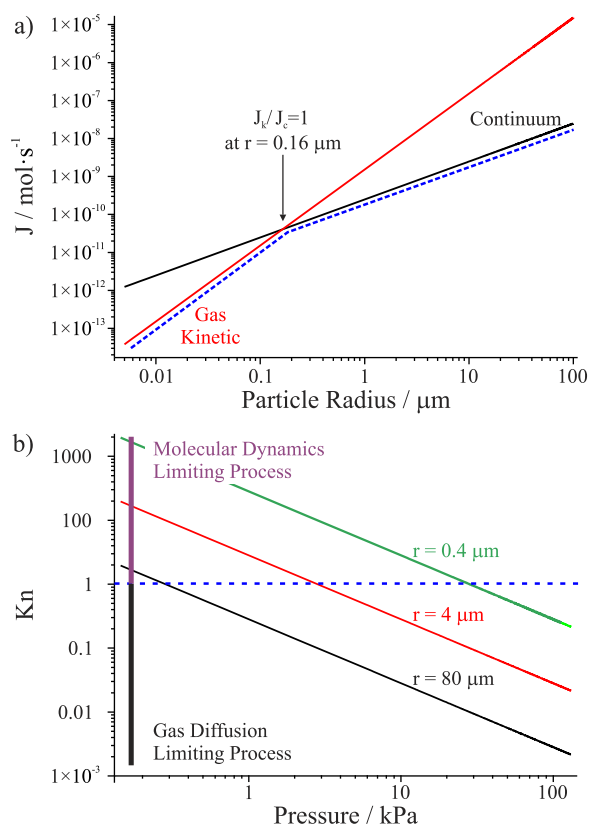


FIG. 2. (a) Comparison of the size dependence of molar flux for a particle growing by condensation of water calculated using gas kinetic theory (red line) or assuming the droplet follows continuum theory (the Maxwell equation, black line). Further, it is assumed that the diffusion gradient arises from a vapour pressure difference equal to the equilibrium vapour pressure of water at 20 °C. In reality, the molar flux must follow the approximate path shown by the dashed blue line, transitioning at the size indicated when the gas kinetic flux (J_k) and continuum flux (J_c) are equal. (b) The variation in the Knudsen number with gas phase pressure and particle size for three different particle sizes. When $Kn > 1$, the molecular dynamics of processes such as mass accommodation at the droplet surface limit microphysical processes such as condensational growth. When $Kn < 1$, gas diffusional transport is limiting.

molecule regime ($Kn \gg 1$) at all pressures in the atmosphere, and fluxes must be calculated by the Hertz-Knudsen equation or by using transition correction factors to correct the continuum equations.^{29,30} Whereas characteristic time scales for particles to equilibrate with the surrounding gas phase composition may be shorter than 100 μs for particles smaller than 100 nm in diameter at high concentrations of condensable vapours, slow gas diffusional transport can require minutes to establish equilibrium for particles larger than 100 μm , a change of more than 6 orders of magnitude.³¹ Indeed, the slow gas diffusional transport for large particles reduces the significance of interfacial molecular processes and the impact of α_M less than 1, unless it is many orders of magnitude smaller than 1.³²

Particles can grow by condensation, but they can also grow by collision with other particles. Encounters between aerosol particles continuously lead to evolving particle number and size distributions through coalescence.³³ Although significant to the ensemble, the encounter itself may be complete in $<1 \mu\text{s}$, spanning the time from a sufficiently close approach that particles interact to the formation of a composite particle.^{33–35} Assumptions are commonly made about

how coalescence proceeds, often neglecting the interactions that occur, the change in apparent collision cross sections that result, and the probability that two particles merge to form one particle on collision.^{36–38} Interparticle interactions are often dependent on charge interactions: like-charged particles can attract as well as repel and the range of these interactions can be considerably longer than the interactions between charged particles in a solution phase with a high dielectric constant.^{39,40} Despite these complexities and the significance, for example, of coalescence in determining aerosol particle lifetime in the atmosphere, there are very few experimental studies of aerosol coalescence, primarily because of the challenges in studying sporadic transient events.^{12,33–36,38,41–43} Coalescence can even lead to a change in the particle phase.^{44,45} One example of this phenomenon is contact freezing, when a subcooled water droplet encounters an aerosol particle or when a dry crystalline particle makes contact with a supersaturated solution droplet.^{45,46} However, a detailed mechanistic understanding of contact freezing remains elusive.

So far we have considered largely liquid aerosol droplets. Indeed, the common absence of a solid substrate within a liquid droplet leads to the prevalence of metastable solution phases that cannot be formed in the bulk phase, achieving a high supersaturation with respect to the bulk solubility limit.⁷ These solution phases can lead to the formation of ultraviscous liquids and metastable crystalline or amorphous particles,^{47–50} providing unique opportunities in particle synthesis^{5,51,52} but also presenting challenges when attempting to understand the role of aerosols in, for example, the atmosphere.^{53–56} Indeed, the dramatic slowing of diffusional transport in increasingly viscous particles, which can be estimated from the Stokes-Einstein equation and the inverse relationship between the dynamic viscosity and diffusion constant,^{12,33} leads to time scales that can even be years for diffusional transport over the lengthscale of a typical particle size!^{11,47} Thus, although typical droplet evaporation time scales may be seconds when considering only gas phase transport, slow bulk phase diffusion may in fact increase the time scale beyond any reasonable experiment. Recently, this has led to an interesting intersection between the chemical physics research domains of aerosols, glass formation, nucleation, and crystallisation. In addition, such slow dynamics could even be responsible for the slow chemical transformation and oxidation of atmospheric aerosols^{57–60} and the long-range transport of chemical pollutants,^{61–63} placing a chemical physics problem at the focus of an environmental issue.

Having established the time scales and lengthscales relevant for a range of microphysical processes, we now move progressively from clusters to surfaces to bulk phases, exploring in more detail the chemical physics central to aerosol dynamics.

III. NEW PARTICLE FORMATION AND GROWTH

A longstanding problem in atmospheric aerosols is the production of new particles.^{64,65} New particle formation is largely driven by the photochemical production of gaseous sulfuric acid^{66,67} and/or low volatility organic molecules.⁶⁸ New particle formation increases the total number of atmospheric

particles that may serve as cloud condensation nuclei (i.e., cloud droplet seeds) and, in fact, may contribute up to 50% of cloud condensation nuclei.⁶⁹ An increase in the cloud droplet number concentration changes cloud reflectivity as well as precipitation patterns.⁷⁰ Atmospheric new particle formation can be subdivided into two processes. The first process is the homogeneous nucleation of stable clusters from gas phase precursors.^{71,72} The second process is the growth of those stable clusters to larger sizes. Nucleation ultimately determines the total number of particles that may be formed. Growth largely determines whether the nucleated particles will have a climatic impact. In order for nucleated particles to become climatically relevant, they must rapidly grow to 50-100 nm diameter.^{66,73}

The key molecules contributing to new particle formation include sulfuric acid, ammonia, amines, organic molecules, and water although the chemical physics underlying the process is poorly understood. For example, classical nucleation theory tends to do poorly at predicting the number of nucleated particles, likely due to the chemical complexity of the system.^{26,74} Similarly, particle growth is often significantly faster than that expected based on known condensational processes.⁷⁵⁻⁷⁷

One area where our understanding of new particle formation has advanced significantly is the competition between ammonia and amines in initial growth of acid-base clusters (typically, sulfuric acid and a base). In the atmosphere, ammonia is typically 100-1000 times more abundant than amines (low ppb vs. low ppt). However, amines have been observed in ambient sulfuric acid-containing nanoparticles and clusters despite their low concentrations.^{78,79} Additionally, in well characterised particle formation experiments, dimethylamine was observed in molecular clusters despite only ammonia, sulfuric acid, and water being intentionally introduced to the chamber.¹⁶ Further experiments indicated that particle formation in the amine-sulfuric acid-water system proceeds in a roughly collision limited manner, unlike observations for the ammonia-sulfuric acid-water system.⁸⁰⁻⁸² These observations are significant because they indicate that in the atmosphere, amines can potentially outcompete ammonia at forming and growing clusters, thereby enhancing particle number concentrations and their climatic impacts relative to expectations based on ammonia.

The fundamental chemistry underlying the competition between amines and ammonia in salt clusters is an instructive example of how physical chemistry and chemical physics can clarify the processes underlying important atmospheric phenomena.¹⁵ For example, a study of size- and composition-selected charged ammonium bisulfate clusters examined their fragmentation energetics using a Fourier transform mass spectrometer equipped with surface induced dissociation.⁸³ The relative abundances of the fragment ions resulting from the collision were monitored in a time- and collision-energy-resolved manner. The energetics of cluster fragmentation were quantified using a Rice-Ramsperger-Kassel-Marcus/quasi-equilibrium theory model and interpreted under the assumption of microscopic reversibility (i.e., cluster growth is the reverse of fragmentation). The experimental energies were compared to computationally calculated energies, and if the

experimental energy for a particular fragmentation step was larger than the calculated energy, an activation barrier to the reverse (i.e., addition) step was implied. The key results for two experimentally studied clusters are illustrated in Fig. 3(a), with the fragmentation pathway illustrated from left to right in the figure. First, positively charged ammonium bisulfate clusters fragment primarily through stepwise loss of ammonia followed by loss of sulfuric acid. This observation indicates that cluster growth (reading from right to left in the figure) proceeds first through the addition of sulfuric acid followed by neutralisation by ammonia. Second, the energetic results indicate that there may be a substantial barrier to the ammonia addition but a minimal barrier to the sulfuric acid addition, as a higher E_0 for ammonia loss is measured relative to computation but the measured E_0 for sulfuric acid loss agrees with computation. This observation is consistent with kinetic measurements of ammonia addition to charged bisulfate clusters, which determined reaction probabilities $<10^{-3}$.⁸⁴ Computational modelling of the cluster growth pathway suggests that the activation barrier to ammonia addition could arise from a charge separation induced by the approach of ammonia's lone pair electrons in the pre-association complex followed by a substantial structural rearrangement to accommodate the proton transfer from sulfuric acid to ammonia (forming ammonium and bisulfate).⁸⁵ Linear action spectroscopy of these clusters also indicates a substantial rearrangement in structure for a cluster containing ammonium relative to the one without ammonium.⁸⁶ The concept of an activation barrier to cluster growth in the ammonia-sulfuric acid system, whether kinetic or thermodynamic,¹⁸ is consistent with observations of non-collision limited cluster growth.

In order to better understand the mechanisms by which bases are incorporated into growing clusters, additional experiments examined reactions of charged ammonium bisulfate clusters with gas phase ammonia and amine, also using Fourier transform mass spectrometry.^{84,87-89} Figure 3(b) shows a mass spectrum 12 s after the start of a reaction of the negatively charged cluster $[(\text{NH}_4^+)(\text{HSO}_4^-)_2(\text{H}_2\text{SO}_4)_3]^-$ with dimethylamine gas.⁸⁴ From the mass spectrum, it is apparent that a substantial reaction has occurred. Figure 3(c) shows a reaction profile, which visualises the time-dependent progress of the reaction. The lines are fits of the experimental data to pseudo first order kinetics. It is clear from the reaction profile that two pathways exist for the incorporation of bases into molecular clusters. The first pathway is by displacement of the pre-existing base (cluster **A** to cluster **B**), which occurs very quickly (reaction probability ~ 1). The second pathway is by neutralisation of sulfuric acid (cluster **B** to **C**, **C** to **D**, and **D** to **E**), which occurs more slowly than displacement, especially for ammonia (reaction probabilities with $\text{NH}_3 < 10^{-3}$). The slow neutralisation step is consistent with the concept of an activation barrier discussed above. Further experiments showed that displacement is generally highly efficient on the cluster surface (reaction probabilities ~ 1) but slows significantly in the cluster core (reaction probabilities $<10^{-3}$).^{84,87-89} The favourability of displacement correlates with the gas phase basicity of the incoming base.⁸⁸ A similar trend was observed in the stabilisation of uncharged sulfuric acid dimers by

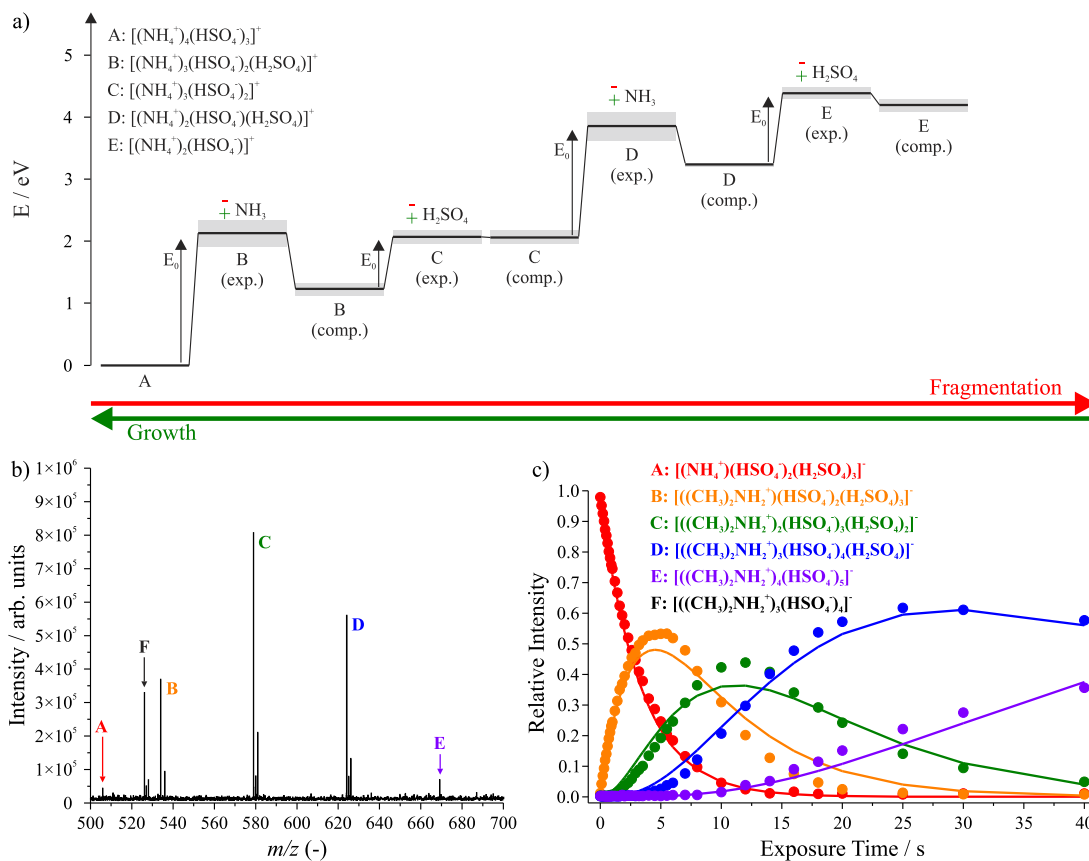


FIG. 3. (a) Potential energy surface for fragmentation of a positively charged ammonium bisulfate cluster. Fragmentation occurs first by loss of ammonia followed by loss of sulfuric acid. Assuming microscopic reversibility, cluster growth would be the reverse process (right to left across the figure). Energetics are indicated for experiment (“exp.” indicated by the arrow labeled E_0) and computation (“comp.”). If no activation barriers are present, fragmentation proceeds from one thermodynamic value to the next [i.e., “A” to “B (comp.)” etc.]. If activation barriers are present, the experimental energy will be larger than the corresponding computational energy. Gray boxes show the experimental or computational uncertainties. (b) Mass spectrum 12 s after the start of the reaction of $[(\text{NH}_4^+)(\text{HSO}_4^-)_2(\text{H}_2\text{SO}_4)_3]^+$ [cluster A, defined in (c)] with dimethylamine gas, indicating the formation of a number of products. (c) Reaction profile visualising time dependent relative ion abundances for precursor and product clusters. Symbols are experimental values. Lines are fits to pseudo first order kinetics. Each colour denotes a different reaction step. Cluster assignments in (c) also correspond to (b). Adapted with permission from Bzdek *et al.*, *Acc. Chem. Res.* **50**, 1965 (2017), which is an adaptation from Refs. **83** and **84**. Copyright 2017 American Chemical Society.

different bases.¹⁷ However, computational modelling of aminium bisulfate and ammonium bisulfate clusters indicates that displacement energetics are far less exergonic than expected based solely on differences in gas phase basicity.⁸⁵ Although amines are more basic than ammonia, aminium bisulfate clusters have less favourable interaction strengths than ammonium bisulfate clusters because ammonia has more protons available for binding and can create a tighter packing of cations and anions. Therefore, the competition between amines and ammonia in small molecular clusters is governed by the trade-off between gas phase basicity and binding energetics, which ultimately suggests that amines would be favoured in the smallest clusters but not in the larger ones.¹⁵ The overarching conclusion of amine-ammonia competition in new particle formation is that amines may be key in assisting the initial formation and growth steps but become less significant as clusters grow to larger sizes.¹⁵

More recently, attention has focussed on the role of low volatility organic molecules in particle formation and growth.^{90–92} Oxidised organic molecules have been implicated in the formation of particles via clustering with sulfuric acid⁹³ as well as via clustering with other organic molecules.⁹⁴

Extremely low volatility organics, which may be highly oxidised, have been shown to drive cluster and nanoparticle growth.^{95–97} The existence of these highly oxidised molecules was rationalised through an autoxidation mechanism, which is well known in liquid phase chemistry but previously underappreciated in gas phase chemistry. This mechanism is now known to be operative in the oxidation of the two most abundant atmospheric monoterpenes: limonene and α -pinene.⁹⁸ Figure 4(a) illustrates an example autoxidation pathway: the ketone **C1** is converted into the dicarbonyl hydroperoxide **C2**, with OH serving as a catalyst. By this mechanism, inter and/or intramolecular hydrogen abstraction by peroxy radicals begins a chain reaction of hydrogen shifts and O_2 incorporation to give a final product containing hydroperoxide and carbonyl functionalities.⁹⁹ Mentel *et al.* systematically studied the ozonolysis of a series of alkenes with endocyclic double bonds and through comparison of the reaction products produced from different initial compound structures concluded that the produced molecules are highly oxidised, multifunctional percarboxylic acids, with carbonyl, hydroperoxy, and hydroxyl groups incorporating in the terminal steps of oxidation.¹⁰⁰ The rate of hydrogen abstraction is highly sensitive

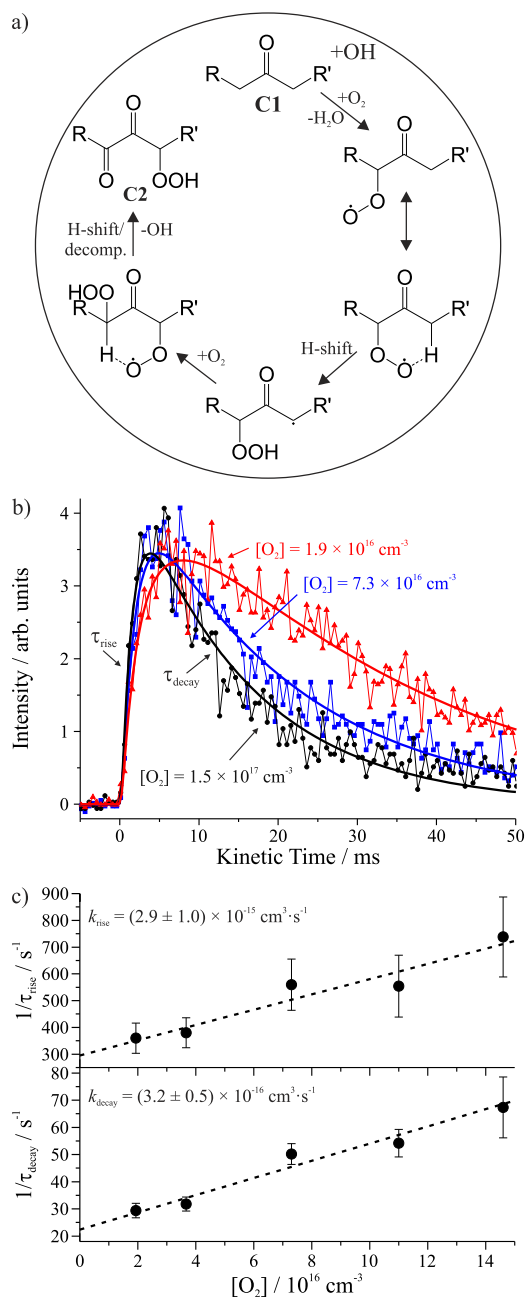


FIG. 4. (a) Example autoxidation scheme. (b) Time dependence of the hydroperoxyalkyl radical mass spectrometric signal obtained at 8.3 eV at different $[O_2]$ (line-symbol traces) along with the corresponding double exponential fits (solid lines). (c) Second-order plots showing the linearity of $1/\tau_{\text{rise}}$ and $1/\tau_{\text{decay}}$ versus $[O_2]$ and the accompanying linear fits. The slope of the fits gives k_{rise} and k_{decay} , which are assigned as rate constants for the consumption and production of the hydroperoxyalkyl radical, respectively. Part (a) is adapted with permission from Crouse *et al.*, *J. Phys. Chem. Lett.* **4**, 3513 (2013). Copyright 2013 American Chemical Society. Parts (b) and (c) are adapted with permission from Savee *et al.*, *Science* **347**, 643 (2015). Copyright 2015 AAAS.

to neighbouring substituents.⁹⁹ As a result, the rate of reaction increases rapidly as more oxygen containing functionalities are added to the molecule. Yields of these reactions are expected to be on the order of only a few percent,¹⁰¹ but this is sufficient to boost substantially the growth of the nucleated clusters.

Although the basic premise of autoxidation is understood, reaction rates for the individual steps are poorly constrained.

On the whole, the reaction appears very fast, resulting in products formed within just a few seconds,¹⁰¹ consistent with the particle phase observation of high molecular weight products in aerosols shortly after the start of the reaction.¹⁰² To date, only a few measurements of the kinetics for intermediates along the reaction pathway, for instance, hydroperoxyalkyl radicals, have been performed.^{103,104} Figure 4(b) shows one experiment where reaction rates were measured.¹⁰³ In this experiment, a hydroperoxyalkyl radical intermediate in the oxidation of 1,3-cycloheptadiene was isolated and reacted with O_2 . The reaction kinetics were monitored by photoionisation mass spectrometry, where the ionisation was accomplished with synchrotron-generated tunable vacuum ultraviolet radiation. Mass spectrometry allowed observation of a transient reaction product at the mass-to-charge ratio corresponding to the hydroperoxyalkyl radical, and photoionisation spectra allowed confident identification of the radical, based on the high agreement between the observed and expected adiabatic ionisation energies. Figure 4(b) shows the time dependence of the hydroperoxyalkyl radical as a function of oxygen concentration at a photoionisation energy of 8.3 eV. The data were fit to a double exponential kinetic model, giving time constants for the rise (τ_{rise}) and decay (τ_{decay}) that are linear with $[O_2]$, which was maintained in excess. This approach allowed quantification of the rate constants k_{rise} and k_{decay} [Fig. 4(c)]. Further experiments and modelling demonstrated that k_{decay} corresponds to the rate constant of hydroperoxyalkyl radical formation, whereas k_{rise} corresponds to the rate of radical consumption.¹⁰³ The relatively slow rate constants indicate that this particular hydroperoxyalkyl radical is long-lived due to doubly allylic resonance stabilisation of the radical (owing to its provenance from the unsaturated cycloheptadiene). Because many organic aerosol precursors are unsaturated (e.g., α -pinene), these hydroperoxyalkyl radicals may be relatively long-lived in the atmosphere.

The role of organic molecules in new particle growth is still progressing. While the elemental composition of many highly oxidised atmospheric molecules is known, their molecular structure has yet to be fully resolved, and it is not clear which of the products are responsible for cluster and nanoparticle growth, as not all products are expected to have sufficiently low volatility to promote growth.^{105,106} Additionally, higher volatility products have been hypothesised to promote growth not by condensation but instead by adsorbing (due to intermolecular forces) onto the cluster surface, thereby increasing the size of the cluster, significantly decreasing the equilibrium vapour pressure, and reducing the minimum saturation ratio required for the organic molecule to contribute to growth.¹⁰⁷

It is also important to understand the fate of molecules once they partition to clusters and nanoparticles. Once contained within a cluster or particle, non-volatile and semi-volatile molecules undergo further chemistry. For example, semi-volatile molecules may become non-volatile via condensed phase accretion reactions and further promote particle growth.¹⁰⁸ If such chemistry is operative, a particle size dependence in composition would be apparent, as the relative contributions of condensation (a surface process) and reaction (a bulk process) vary with particle size. A few recent

studies have uncovered size dependent chemistry that bares out this premise and is a direction for future work.^{109–111} However, low volatility oligomeric molecules commonly present in organic aerosols may also rapidly react with oxidants like OH¹¹² or may photodegrade¹¹³ to produce potentially more volatile monomeric products.

IV. THE AEROSOL PARTICLE SURFACE

The properties of aerosol particle surfaces are known to be important in a variety of key atmospheric processes and to the rates of heterogeneous reactions. For example, an atmospheric particle's surface tension helps determine the critical supersaturation in relative humidity (RH) that must be surpassed for a particle to grow into a cloud droplet.¹¹⁴ A high surface tension results in a high critical supersaturation and fewer cloud droplets are formed. A low surface tension results in a lower critical supersaturation, resulting in a substantial increase in the cloud droplet number concentration that increases cloud reflectivity and decreases precipitation. Additionally, reactions on mineral dust surfaces^{115,116} and ice particles¹¹⁷ are key to many climate processes, including nitrate and sulfate photochemistry^{118,119} and, of course, formation of the ozone hole.¹²⁰ Chloride ion concentrations may be enhanced at the interface of aqueous sea salt particles, allowing reactions that are fundamentally different in terms of kinetics and mechanism to those occurring in the particle bulk.¹²¹ Reactivity near or on the particle surface depends on parameters like reaction rates, surface concentrations, and bulk diffusion constants, which may all impact the reacto-diffusive length.^{122–125} Indeed, efforts to infer the surface propensity and orientations of molecules and ions at the particle-air interface have been underway for years.^{126,127} However, these approaches typically involve surface specific spectroscopies, such as second harmonic generation, sum frequency generation, X-ray photoelectron spectroscopy, and ion scattering, which usually require bulk samples or a continually renewed surface for analysis.^{125,128–135} Bulk solutions are unable to access the range of compositions attainable in aerosol droplets and may not accurately represent gas-particle partitioning due to the high surface-to-volume ratio present in aerosols. Therefore, most approaches to resolve the particle-air interface through direct study of aerosols often rely on indirect measures of the surface composition.

One of the indirect approaches is to study the evaporation or hygroscopic growth of aerosols, i.e., to use the dynamics of molecular transfer across the interfacial region as a tool to infer the character of the surface. For example, highly oriented condensed films formed by insoluble long chain alcohols [$C_nH_{2n+1}OH$] reduce the evaporation coefficient of a water droplet by several orders of magnitude.³² Figure 5 illustrates this concept for tridecanol (gold line) and pentadecanol (black line). When the alcohol-doped aqueous droplet is injected into a RH controlled cell, an initial decrease in radius with time arises from the evaporation of ethanol used to solubilise the alcohol in the droplet (<1 s). This initial ethanol loss is followed by swift water loss during the first 10 s. When the droplets are around 15 μm radius, droplet radius begins to decrease linearly with evaporation time. This linear decrease

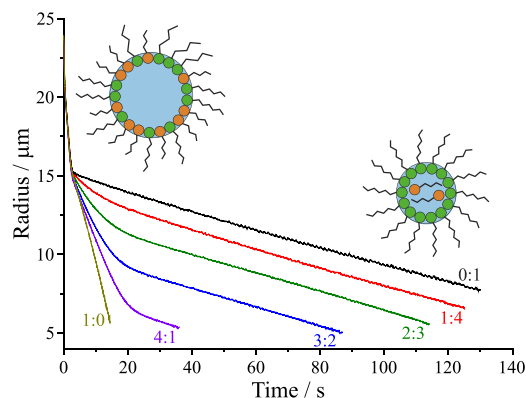


FIG. 5. Time-dependent change in the droplet radius for aqueous droplets doped with tridecanol (gold), pentadecanol (black), and different tridecanol:pentadecanol molar ratios. These droplets are evaporating into 60% RH at 293.15 K. Monolayer film formation is observed at ~ 15 μm radius for all droplets. The pictorial description illustrates that the more soluble alcohol (tridecanol) moves into the bulk as the droplet evaporates, leaving the less soluble alcohol (pentadecanol) on the surface. Adapted with permission from Miles *et al.*, Phys. Chem. Chem. Phys. **18**, 19847 (2016). Copyright 2016 PCCP Owner Societies.

in radius over time results from the formation of a condensed film of long chain alcohols on the surface (as quantified by an inferred surface area per alcohol molecule on the order of 20 \AA^2) that dramatically inhibits evaporation. This observation is in contrast to uninhibited evaporation (e.g., for pure water droplets) where radius-squared decreases linearly with evaporation time. The inhibited evaporation rate scales with the chain length of the alcohol, with longer chain lengths corresponding to lower evaporation rates.³²

When mixtures of insoluble long chain alcohols in aqueous droplets are studied, evaporation is initially slowed by a combination of the different alcohols.¹³⁶ However, as evaporation continues, the rate of evaporation changes to a value consistent with that of the less soluble alcohol. For example, in Fig. 5, the rate of evaporation of 4:1 tridecanol:pentanol droplets (purple line) changes at ~ 20 s and equals that of pure pentadecanol (black line). As droplet surface area diminishes, the more soluble alcohol (here, tridecanol) partitions to the droplet bulk, whereas the less soluble alcohol (pentadecanol) remains at the surface, forming a condensed film and further slowing evaporation to a rate equivalent to that expected if it were the only component at the droplet surface. On the other hand, condensation of water onto a droplet containing a condensed film is not inhibited, as strong cohesive forces among the long chain alcohol molecules lead to islands forming as the droplet grows, opening up uncoated areas onto which water may rapidly condense.³² One implication of these observations is that atmospheric aerosols are unlikely to experience inhibited evaporation because of the requirement that the surface film be a condensed coherent film. The chemical complexity of atmospheric aerosols suggests that it is unlikely a coherent film would occur naturally in aerosols.

Measurements of the hygroscopic growth of aerosol particles when RH is increased can also be used to infer the surface composition of a particle. For example, through the Köhler theory, the hygroscopic growth of a particle allows the estimation of the surface tension of the particle, but only at high RH ($>95\%$) where the surface tension term becomes

significant and for particles that are sufficiently small that the surface curvature has a significant impact on the droplet vapour pressure (typically <200 nm diameter).^{137,138} A recent series of experiments examined the hygroscopic growth of an aerosol containing an inorganic salt core and an organic coating.^{13,139,140} Examination of the hygroscopic growth in the RH range 99.2%-99.9% (i.e., the increase in the particle size relative to that at 0% RH) indicated that particles containing an aqueous NaCl core and a shell composed of α -pinene ozonolysis products have surface tension 50%-70% lower than that of pure water, but only if the humidified droplet shell has a thickness of approximately 0.8 nm, or around a monolayer.¹³⁹

Further work systematically inferred the impact of the molecular makeup of the monolayer film on the droplet size,¹⁴⁰ not dissimilar to the examination of the role of the phase of the monomolecular film on evaporation rates discussed above. In these experiments, particles containing an ammonium sulfate core and a model organic compound shell of varying thickness were examined. The model organic compounds were mono and di-carboxylic acids of different chain lengths. The measured droplet size at 99.9% RH was related to the structure of the model organic compound and to the dry particle shell thickness. The wet droplet size exhibited a complex, nonlinear dependence on the organic fraction, which was explained only by considering the two-dimensional van der Waals equation of state. Insoluble mono- and di-carboxylic acids were shown to partition to the surface (thereby reducing surface tension) upon formation of a two-dimensional condensed monolayer. The dependence of shell thickness (threshold organic fraction) on the diacid structure is illustrated in Fig. 6.¹⁴⁰ The symbols represent the minimum organic fraction required to observe a change in the hygroscopic growth relative to that of pure ammonium sulfate particles. For diacids, the ability to form a condensed monolayer depended on whether the acid contained an even or an odd number of carbon atoms. Modelling of these experimental data with the 2-D van der Waals model attributed the differences to the much smaller

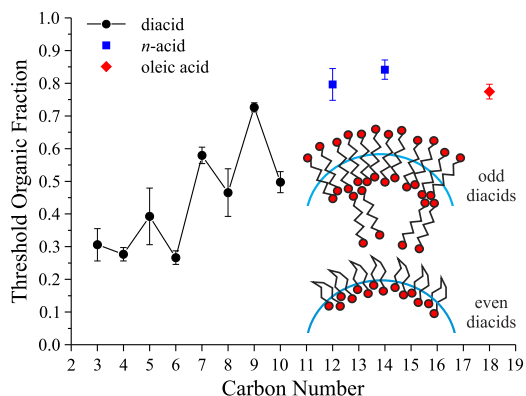


FIG. 6. The threshold organic volume fraction (which correlates to a shell thickness) at which hygroscopic growth measurably changes from the bare ammonium sulfate seed. The graphic illustrates the difference in the surface film structure between the odd and even carbon number diacids, which explains the experimental results. Adapted with permission from C. R. Ruehl and K. R. Wilson, *J. Phys. Chem. A* **118**, 3952 (2014). Copyright 2014 American Chemical Society.

molecular areas of the odd carbon number diacids ($\sim 20 \text{ \AA}^2 \text{ molecule}^{-1}$) compared to the even carbon number diacids ($\sim 40 \text{ \AA}^2 \text{ molecule}^{-1}$). This conclusion, illustrated conceptually in Fig. 6, suggests that the even carbon number diacids bend around to form “folded films” where both carboxylic acids are in contact with the aqueous phase (thereby requiring fewer molecules, or a smaller organic fraction, to form a film), whereas the odd carbon number diacids are more tightly packed with only one carboxylic acid group contacting the aqueous phase.

Hygroscopicity measurements at high RH also resolved key discrepancies in our understanding of how particles grow into cloud droplets. Additional experiments showed that at the critical supersaturation at which a particle activates as a cloud droplet, droplet diameters were $\sim 50\%$ larger than those predicted by the Köhler theory, resulting from a particle surface tension much less than that of pure water up to the point of activation.¹³ However, beyond activation, droplet growth proceeded in agreement with expectations (which assumes a surface tension equivalent to that of pure water). This observation was consistent with the compressed film picture discussed above; up to the point of activation, the initially compressed film lowers surface tension, but beyond it, the film transitions to a gaseous state with surface tension approaching that of pure water.

The examples discussed above provide only indirect information about the surface composition of aerosol particles, with molecular detail derived through measurements of their hygroscopic growth or evaporation rates. Efforts are now underway to more directly understand the particle-air interface. A number of approaches have been applied to study the surface composition of individual aerosol particles and ensemble aerosols, for instance, using X-ray photoelectron spectroscopy,^{141,142} near edge X-ray absorption fine structure,¹⁴³ and second harmonic scattering.¹⁴⁴ Additionally, approaches to measure the surface tension of aerosols have recently been developed. One off-line approach relies on probing individual sub-micrometre aerosol particles collected onto a substrate with the tip of an atomic force microscope.¹⁴⁵ By measuring the recoil force as the tip is pulled out of the particle, surface tension is inferred. Another approach is to monitor the coalescence dynamics of two optically trapped droplets.³³⁻³⁵ As illustrated by the images in Fig. 7(a), coalescence of low viscosity droplets proceeds through damped oscillations in droplet shape. These shape oscillations are monitored by elastic backscatter from the laser light used to optically trap the coalescing droplets. A typical experimental trace is shown in Fig. 7(b), along with the aspect ratios from the images in Fig. 7(a). Elastic backscattered light allows for higher time resolution monitoring of the shape oscillations relative to camera images. The square of the frequency of the shape oscillations is proportional to the droplet surface tension. This approach enables a precise measurement of the equilibrium surface tension of droplets, as illustrated in Fig. 7(c),^{35,146} allowing direct measurements of the surface tension of picolitre volumes even beyond the bulk solubility limit^{35,147} and testing of models that predict aerosol surface tension.¹⁴⁶

Future challenges include quantifying the dynamic surface tension of aerosol particles, which has been suggested to

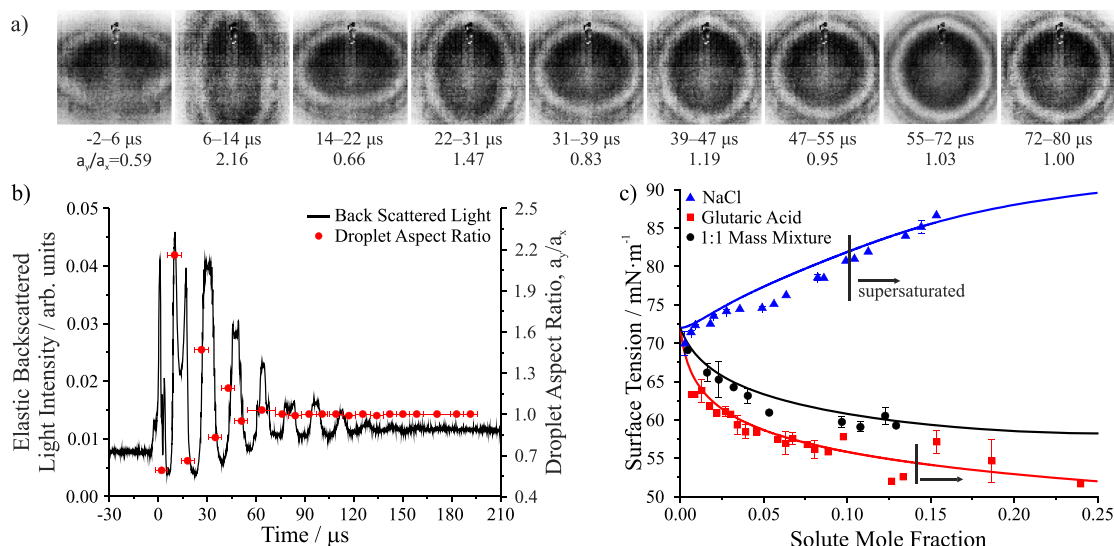


FIG. 7. (a) High frame rate images of the first 80 μs after coalescence of two aqueous sodium chloride droplets doped with the surfactant sodium dodecyl sulfate. (b) Elastic backscattered light intensity collected after coalescence (left axis) and droplet aspect ratios from the high frame rate images in part (a) (right axis). Time $t = 0 \mu\text{s}$ corresponds to the moment of coalescence. (c) Measurements of picolitre droplet surface tension for sodium chloride, glutaric acid, and a 1:1 mass mixture of the two compounds (symbols) compared to a statistical thermodynamic model of surface tension (lines). Measurements to the right of the vertical lines for sodium chloride and glutaric acid indicate measurements made on droplets above the bulk solubility limit. Parts (a) and (b) are adapted with permission from Bzdek *et al.*, Chem. Sci. **7**, 274 (2016). Copyright 2016 The Royal Society of Chemistry. Part (c) adapted with permission from Boyer *et al.*, J. Phys. Chem. A **121**, 198 (2017). Copyright 2017 American Chemical Society.

be important to understanding the dynamics of atmospheric aerosol particle size.¹⁴⁸ Additionally, a better understanding of how surfactant molecules partition to the particle surface is required, recognising the finite size of particles. Models predict that the high surface-to-volume ratio in aerosol droplets results in a substantial fraction of the total surfactant molecules in a droplet partitioning to the surface, depleting the bulk surfactant concentration, and resulting in a higher surface tension than expected based on a bulk measurement.^{149–153} However, these models remain untested by experiment and simplify the complex composition of aerosols to just one or two components.

V. PROPERTIES AND DYNAMICS IN THE PARTICLE BULK

For solid crystalline particles, it may be appropriate to consider only the processes that occur at the particle surface, as the potential for processes within the particle bulk can be ignored. However, for liquid droplets, amorphous particles, and porous particles, understanding transport processes within the particle bulk during any dynamic process is key when rationalising observations of particle heterogeneity, reactivity, and composition. Changes in the particle composition and size arise in response to changes in gas phase conditions. For example, consider aqueous solution droplets containing solutes. A steady state is attained when the vapour pressure of water at the droplet surface equals the partial pressure of water at infinite distance. If the gas and particle are at the same temperature and neglecting any impact from the surface curvature (i.e., the surface tension effects already discussed), the activity of water in the droplet bulk is in equilibrium with the gas phase RH. Changes in the gas phase RH drive commensurate changes in the water activity within the droplet, leading to a change in

the mass fraction of solute. Figure 8 provides an illustration of this concept for aqueous droplets containing a mixture of non-volatile sucrose and semi-volatile maleic acid, an unsaturated dicarboxylic acid with a vapour pressure, p_{MA}^0 , of $\sim 10^{-3}$ Pa [see Fig. 8(c) for a pictorial description]. These data were collected using aerosol optical tweezers, which allows precise measurements of the size and refractive index of an optically trapped droplet as ambient conditions like RH are modified.^{154–156} At step changes in RH [Fig. 8(a), upper panel], the droplet responds by losing water, with a commensurate step in particle size, leading to higher solute concentrations and a lower water activity. A concomitant increase in the refractive index [Fig. 8(a), lower panel] occurs due to the increase in solute concentration, with sucrose and maleic acid having a higher refractive index than water. An additional change occurs in the droplet size between steps in RH: the droplet size decreases due to the continual evaporation of the semi-volatile maleic acid component, with a commensurate loss of water to maintain the water activity in the droplet equal to the RH.^{154,155} In these experiments, the gas phase is continually purged, removing maleic acid and establishing a concentration gradient from the droplet surface to infinite distance, which leads to the slow volatilisation of maleic acid at a rate governed by its vapour pressure at the solution composition, p_{MA} , which in turn depends on the maleic acid mole fraction, x_{MA} , and the activity coefficient, γ_{MA} ,

$$p_{MA} = x_{MA}\gamma_{MA}p_{MA}^0. \quad (1)$$

This slower change is highlighted in greater detail in Fig. 8(b), which also illustrates the precision in radius and refractive index measurement afforded by the approach. This slower change in the droplet size due to volatilisation can be useful for inferring organic molecule diffusion constants within the particle.^{58,157}

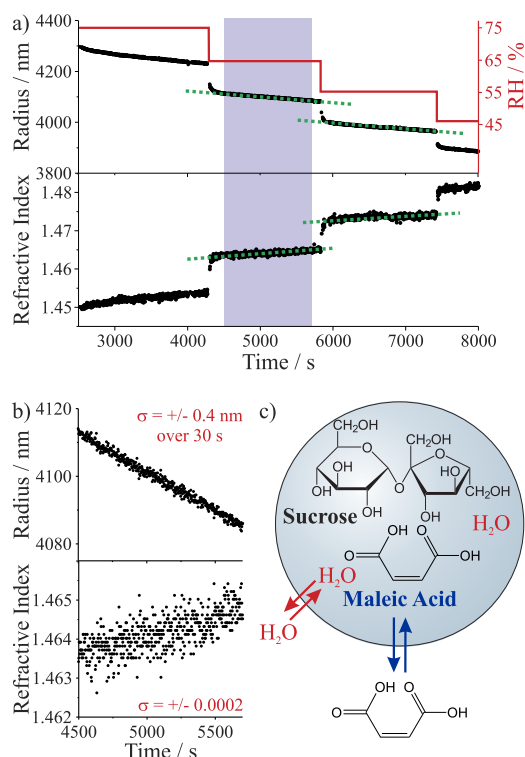


FIG. 8. (a) Responses in radius and refractive index of a droplet containing non-volatile sucrose, semi-volatile maleic acid, and water to step changes in RH (right axis). The green dotted lines highlight the slow change in radius and refractive index due to volatilisation of maleic acid, desorbing with an appropriate equilibrium amount of solvating water, while the droplet is held at constant RH. (b) Expanded view of the slow changes in the droplet radius and refractive index over a 1250 s period of constant RH. The precision of the measurement is highlighted by the embedded text. (c) Illustration of the dynamics of the droplet components.

Underlying this simple example are some interesting challenges in the chemical physics of aerosols. At the RHs/water activities of the experiment shown, maleic acid and sucrose are supersaturated with respect to their bulk concentrations. As already described, supersaturation of solutes is typical of aerosol systems, with the aerosol remaining in a metastable liquid phase when a crystalline phase is energetically preferred.⁷ Indeed, as the RH and water activity approach zero, the droplet may correspond to a subcooled liquid or melt.¹⁴ Such behaviour has been observed even for inorganic salt solutions. For example, there are numerous reports of sodium nitrate droplets existing under dry conditions without crystallisation,^{158,159} and it is common for organic solution droplets to continuously lose and gain water on decreasing and increasing the RH, respectively, without crystallisation.^{7,48} Even aqueous sodium chloride can achieve a supersaturation >2.2 with respect to the solubility limit before crystallisation occurs.^{160,161} Measurements of the phase state of aerosol particles with varying RH and particle size could provide useful insights for understanding the nucleation of crystalline phases.

Even if crystallisation of solute does occur under dry conditions, the significant supersaturations that are achieved in aerosol droplets lead to strong non-idealities in solution behaviour and activity coefficients that depart significantly from 1.⁷ Measurements can then provide insights into

intermolecular interactions; indeed, there is a pressing need to better quantify and treat the interactions between charged inorganic ions and uncharged organic solutes. There are very few measurements that have examined the veracity of model predictions of equilibrium solution composition for highly complex mixtures involving many components and classes of species,¹⁶² where there may be many different types of intermolecular interactions and molecular species forming a solvated network.

More generally, understanding the equilibrium response in solution composition to RH is key to variation in aerosol particle size. In a very recent paper, uncertainties in the hygroscopic response of low solubility organic aerosols have been shown to lead to significant uncertainties in the direct and indirect radiative forcing of aerosols, even to the level of comparability between the uncertainty and the best estimate of the magnitude of the effect.¹⁶³ Although the water activity in solution droplets must approach 1 in the dilute limit, predicting the level of hygroscopic growth at high RH for insoluble organic aerosols used in inhalation therapies as well as for atmospheric aerosols is challenging.^{164–169} In addition, the example in Fig. 8 illustrates that refractive indices of aerosols, essential for quantifying the radiative impact in the atmosphere, must be measured in the aerosol phase; measurements in bulk solution phases are unable to achieve the compositions that can be achieved in aerosols.⁷

In many instances, the partitioning of components between the gas and condensed phase is uncertain due to uncertainties in the pure component vapour pressures, not just the appropriate activity coefficients.¹⁴ In an atmospheric context, organic components with vapour pressures below 10^{-2} Pa are classified as semi-volatile and components with vapour pressures below 10^{-5} Pa are classified as low volatile. Indeed, high molecular weight oligomers formed by chemistry in the aerosol phase have been suggested to have vapour pressures $\ll 10^{-10}$ Pa.^{170,171} A key problem is that such low values are unlikely to ever be measurable. Even for maleic acid, a vapour pressure of 10^{-3} Pa leads to a mass flux of only 0.3 fg s^{-1} for a $5 \mu\text{m}$ radius particle or a change in size of little more than 10 nm in 1000 s. As a consequence, measurements of the vapour pressures of heavily oxidised, low volatility compounds such as citric acid, with functionalities and an O:C ratio typical of organic components in ambient aerosol, span 6 orders of magnitude across different techniques.¹⁷¹ Instead, estimates of vapour pressure must rely on predictive models trained to specific subsets of compounds and chemical functionalities, which can often incur large errors.¹⁷² In addition, aerosol chemical composition is complex and often does not provide molecular specificity in any quantitative manner, making it even more difficult to model ambient aerosol vapour pressures. Clearly, this presents a significant gap in knowledge: to model the mass concentration of aerosols in a polluted urban environment, a key indicator of air quality and airborne particulate matter, the volatility distribution must be constrained.¹⁷³ In many cases, there is just insufficient underpinning of a fundamental physicochemical property such as vapour pressure with which to rationalise and generalise predictive models. In addition, every change in RH must be followed by a readjustment of the gas-particle partitioning of the organic components,

potentially requiring the co-condensation of an organic vapour with water into the condensed phase mass as the RH increases.¹⁷⁴ In order to address this knowledge gap, new and existing techniques to measure volatility must be compared or standardised such that their optimal operational regimes are assessed, similar to recent work by Krieger *et al.*¹⁷⁵ Additionally, better quantification of the relationships among approaches that measure the thermal desorption of aerosol, aerosol volatility, and chemical composition changes that result from thermal desorption is required.¹⁷⁶

So far we have considered fully miscible components. However, for such highly complex mixtures as those found in atmospheric aerosols, it is possible that a single particle may be composed of multiple phases, consisting of either partially dissolved solids or liquid-liquid phase separation.^{177,178} Recent studies have suggested that for ambient secondary organic aerosol particles at high RH/water activity, the equilibrium adopted may consist of phase separated hydrophobic and aqueous phases.¹⁷⁹ Once two aerosol distributions mix, for example, when the aerosol from natural and anthropogenic sources meet, time scales for full readjustment of the partitioning of material between gaseous, hydrophobic, and hydrophilic phases could require hours.¹⁸⁰ The morphology of the resulting particles may also be challenging to predict, with core-shell and partially engulfed structures plausibly depending on surficial and interfacial tensions of the different domains.^{181–183} Indeed, the morphology has been shown to depend on the drying rate for sub-micrometre sized particles typical of the atmosphere.¹⁸⁴ Additionally, a recent study suggested that the liquid-liquid phase separated particles in the atmosphere may reduce the barrier to cloud droplet activation by reducing the particle surface tension, thereby substantially increasing the total number of cloud condensation nuclei.¹⁸⁵

As illustrated in Fig. 8, the partitioning of semi-volatile components between the particle and gas phases requires time, simply due to the small concentration gradients established in the gas phase for low volatility components. By contrast, the adjustments in condensed phase water to changes in RH can be quick, typically complete on time scales <5 s for particles smaller than $10 \mu\text{m}$ diameter.^{162,186} Notably this time scale is comparable to inhalation/exhalation time scales for aerosols into the respiratory tract, opening up the possibility that the inhalation aerosol may never achieve a steady size distribution and suggesting that quantifying rates of condensation and evaporation, and understanding the factors that control these mass fluxes, must be understood.^{164,187}

The increasing mass fraction of solutes that occurs as a particle is dried, as well as reflecting the slowness of nucleation and crystallisation, can lead to substantial increases in particle viscosity.^{12,158,188} However, aerosol particle viscosity is a challenging parameter to measure due to the small sample volumes involved as well as the ability for aerosols to easily achieve supersaturated (and potentially highly viscous) states. One approach to measure aerosol viscosity involves monitoring the coalescence of two droplets and is analogous to the surface tension measurements discussed in Sec. IV.^{12,35} The relaxation time to spherical shape after droplet coalescence is inversely proportional to the viscosity of the composite droplet for low viscosity droplets and is directly proportional to the

viscosity of the composite droplet for high viscosity droplets. In the low viscosity limit, where damped shape oscillations are operative (e.g., Fig. 7), the maxima in the retrieved backscattered light give an exponential decay to a spherical shape, allowing retrieval of viscosity to <0.5 mPa s.³⁵ Above a critical viscosity, coalescence does not proceed through damped shape oscillations but instead proceeds through a merging of the two spheres, as illustrated in Fig. 9 for sucrose droplets across a relatively small RH range (80%-90%).³⁴ Retrieval of the aspect ratios from images of the coalescing droplets allows quantification of the relaxation time through exponential fits, which can span several orders of magnitude, even over a relatively small RH range.

The utility of this approach is highlighted in Fig. 10, where RH-dependent measurements of viscosity for citric acid are plotted.¹⁸⁹ The diamonds illustrate that bulk solution measurements only cover a small range in RH; bulk measurements would be impossible below 80% RH, equivalent to the water activity at the solubility limit. However, in aerosols, the entire RH range can be accessed, with citric acid viscosity increasing by 6 orders of magnitude relative to the viscosity at the bulk solubility limit (80% RH). Figure 10 also illustrates that the viscosity of sucrose aerosol droplets increases over 15 orders

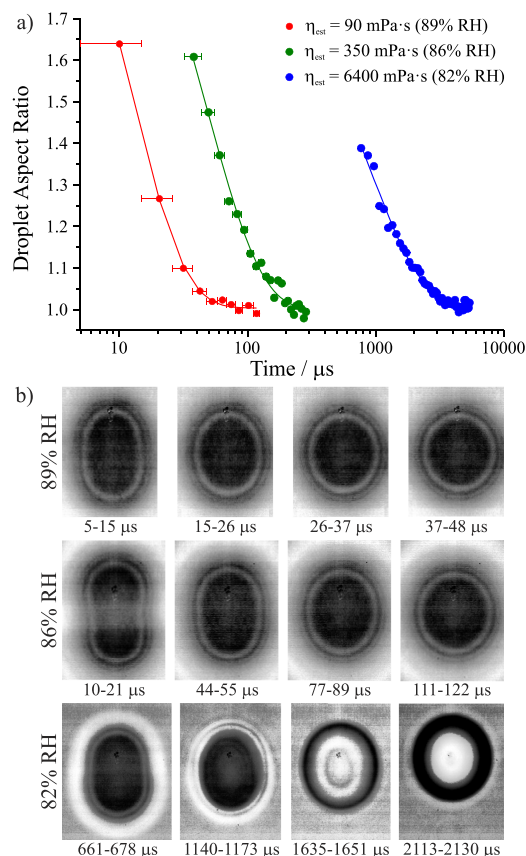


FIG. 9. Coalescence of sucrose droplets at 89%, 86%, and 82% RH, highlighting the order of magnitude time scales inherent to coalescence, even for one system over a relatively small RH range. (a) Droplet aspect ratios from high frame rate imaging of the coalescence. Symbols represent experimentally determined aspect ratios. Solid lines are exponential decays fit to the experimental data. (b) High frame rate images at selected time points during the coalescence events plotted in (a). Adapted with permission from Bzdek *et al.*, J. Chem. Phys. **145**, 054502 (2016). Copyright 2016 AIP Publishing LLC.

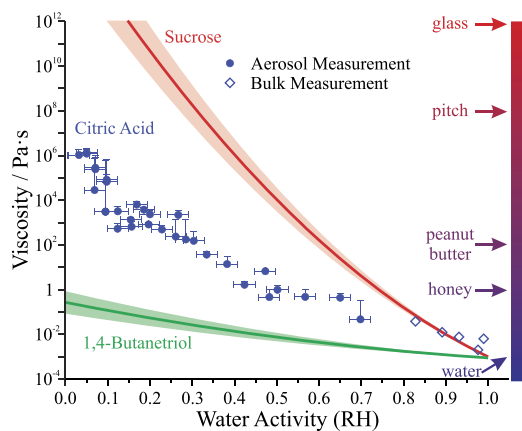


FIG. 10. Measurements of picolitre droplet viscosity across the entire range of RH. Symbols are experimental data points for citric acid.¹⁸⁹ The lines and the corresponding envelopes are fits to droplet measurements and the corresponding uncertainties. A guide correlating various viscosity values to common materials is provided at the right.

of magnitude from 10^{-3} Pa s in the dilute limit to 10^{12} Pa s, equivalent to the formation of a glass at a water activity of ~ 0.2 .^{12,189} Water acts as a plasticiser and can lead to steep variations in particle viscosity with moisture content. From the consideration of the inverse relationship of viscosity and diffusion constant reflected by the Stokes-Einstein equation, it might be expected that this could lead to a commensurate suppression in diffusion constant and, thus, diffusional mixing time scale.^{12,188} In effect, the drying process can be thought to “freeze” the molecular motions and lead to particles that retain moisture on drying purely due to a kinetic constraint. However, the Stokes-Einstein equation breaks down when there is a disparity between the size of the diffusing molecule and the matrix through which it is diffusing.^{12,58,157}

Not only have highly viscous and even glassy particles been observed in atmospheric aerosols, but the suppression of diffusion on the drying time scale is commonly exploited in processes such as spray drying and the formation of heterogeneous particles.^{5,190,191} If the mass flux of evaporating solvent is sufficiently high, the droplet surface recedes sufficiently rapidly that mixing within the droplet volume cannot keep up. This leads to large enrichments in the solute concentration at the particle surface, the formation of a crystalline or amorphous crust, and the formation of hollow or more complex particle morphologies.^{158,192}

In recent work, it has been possible both to determine the viscosity of aerosol particles in metastable supersaturated states as a function of moisture content and to measure the kinetics of water evaporation and condensation following step changes in gas phase RH.^{11,12,58} These latter measurements can be compared with Fickian models of the diffusional kinetics by representing the droplet as a number of concentric shells, albeit assuming ideality in the solution composition.¹⁹³ By comparison with these models, the diffusion constant of water in the pure solute melt can be estimated and the dependence of the diffusion constant on moisture content explored. Thus, these independent measurements of viscosity and diffusion constant can provide insights into the breakdown of the Stokes-Einstein equation and the very diffusional kinetics that initiate nucleation and crystallisation.^{12,158} Recent studies

have confirmed that the Stokes-Einstein equation can provide a first estimate of molecular diffusion constants of large organic molecules diffusing in a viscous matrix, with estimates within 1-2 orders of magnitude of direct measurements. However, as the disparity in molecular sizes becomes more significant (e.g., for water diffusing in a viscous organic matrix), an estimate from the Stokes-Einstein equation can be inaccurate by many orders of magnitude.^{12,58,193,194}

VI. EMERGING CHALLENGES

Aerosols are complex systems requiring a firm understanding of the properties of gas phase molecules (e.g., vapour pressure), small molecular clusters (e.g., growth energetics and kinetics), and large particles (e.g., viscosity). Time scales of aerosol processes can range from nanoseconds (time scale of surface accommodation on a droplet surface) to years (coalescence of two glassy particles). A full understanding of aerosol processes and properties requires application of a wide range of approaches.

Although much progress has been made in our understanding of the chemical physics of aerosols, there are a number of emerging challenges that still require investigation. For example, reactions occurring in aerosols may proceed at much faster rates than in solutions.^{195–199} The underlying reasons for accelerated reaction are not fully understood, but in some cases it may be due to the high surface-to-volume ratio of a particle relative to the bulk,^{198,200} whereas in other cases it may be due to the rapid evaporation of water produced in the reaction.^{197,201} Another emerging research area relates to the study of aerosol acidity,²⁰² which is poorly resolved but helps to govern aerosol chemical processing,²⁰³ phase state,²⁰⁴ and toxicity.²⁰⁵ However, current approaches to infer the pH of aerosols are insufficient,²⁰⁶ in part because the macroscopic definition of pH is no longer valid in sufficiently small particles where the number of water molecules is very limited,²⁰⁷ although some recent advances have been made through Raman spectroscopy of individual particles deposited on a substrate.^{208,209}

One very recent development is the discovery of interfacial photochemistry, often driven by photosensitisers, that can produce a wide range of products that may change the aerosol physicochemical properties as well as release reactive compounds to the gas phase that may even go on to produce new atmospheric particles.^{210,211} A complete understanding of interfacial processes in aerosols will require development of improved approaches to gain chemical and physical insight at the particle-air interface. Photochemistry may also manifest in aerosols through size-dependent reactions resulting from nanofocussing of light in the particle.²¹² Light also impacts aerosol optical properties, and these are often very poorly constrained, especially for particles of heterogeneous composition, as well as for nonspherical and absorbing particles. For instance, a controversial topic is the potential enhancement in absorption cross section resulting from inclusions of black carbon in aerosol droplets.²¹³

In the formulation of aerosols for industrial applications, there remains considerable uncertainty about what governs the final particle structure (e.g., core/shell composition,

morphology, etc.). These final particle properties are likely underpinned by fundamental principles such as the competition between molecular diffusion rates within the particle and evaporation rates.^{52,192,214,215} Similar challenges arise in the formulation of pharmaceutical aerosols, which are engineered to optimise the particle structure for release of the active ingredient as well as optimise deposition in the desired region of the lung.^{166–169} With respect to disease and biosecurity, bioaerosols, which consist of particles containing bacteria and/or viruses coated with secondary species such as organic molecules, are poorly understood. For example, how long bioaerosols remain viable after release, and whether they can mutate in the concentrated environment of aerosols, is currently unknown.^{216,217}

Although aerosols are relevant to a wide range of applications, the fundamentals that govern their properties and processes are similar and are deeply grounded in chemical physics. Improving our understanding of aerosols will require application of the latest advances in chemical physics to this challenging and exciting field.

ACKNOWLEDGMENTS

The authors acknowledge support from the Engineering and Physical Sciences Research Council (EPSRC) through Grant No. EP/L010569/1. B.R.B. acknowledges support from the Natural Environment Research Council (NERC) through Grant No. NE/P018459/1. No new data were created in this study.

- ¹J. Lelieveld, J. S. Evans, M. Fnais, D. Giannadaki, and A. Pozzer, *Nature* **525**, 367 (2015).
- ²J. J. West, A. Cohen, F. Dentener, B. Brunekreef, T. Zhu, B. Armstrong, M. L. Bell, M. Brauer, G. Carmichael, D. L. Costa, D. W. Dockery, M. Kleeman, M. Krzyzanowski, N. Kunzli, C. Liousse, S. C. C. Lung, R. V. Martin, U. Poschl, C. A. Pope, J. M. Roberts, A. G. Russell, and C. Wiedinmyer, *Environ. Sci. Technol.* **50**, 4895 (2016).
- ³B. Forbes, B. Asgharian, L. A. Dailey, D. Ferguson, P. Gerde, M. Gumbleton, L. Gustavsson, C. Hardy, D. Hassall, R. Jones, R. Lock, J. Maas, T. McGovern, G. R. Pitcairn, G. Somers, and R. K. Wolff, *Adv. Drug Delivery Rev.* **63**, 69 (2011).
- ⁴IPCC, Climate Change 2014: Synthesis Report. Contribution of Working Groups I, II and III to the Fifth Assessment Report of the Intergovernmental Panel on Climate Change [Core Writing Team, edited by R. K. Pachauri and L. A. Meyer] (IPCC, Geneva, Switzerland, 2014).
- ⁵R. Vehring, *Pharm. Res.* **25**, 999 (2008).
- ⁶P. H. McMurry, *Atmos. Environ.* **34**, 1959 (2000).
- ⁷U. K. Krieger, C. Marcolli, and J. P. Reid, *Chem. Soc. Rev.* **41**, 6631 (2012).
- ⁸C. D. Cappa, E. R. Lovejoy, and A. R. Ravishankara, *Proc. Natl. Acad. Sci. U. S. A.* **105**, 18687 (2008).
- ⁹V. G. Ciobanu, C. Marcolli, U. K. Krieger, U. Weers, and T. Peter, *J. Phys. Chem. A* **113**, 10966 (2009).
- ¹⁰R. Signorell and M. Jetzki, *Farad. Discuss.* **137**, 51 (2008).
- ¹¹B. Zobrist, V. Soonsin, B. P. Luo, U. K. Krieger, C. Marcolli, T. Peter, and T. Koop, *Phys. Chem. Chem. Phys.* **13**, 3514 (2011).
- ¹²R. M. Power, S. H. Simpson, J. P. Reid, and A. J. Hudson, *Chem. Sci.* **4**, 2597 (2013).
- ¹³C. R. Ruehl, J. F. Davies, and K. R. Wilson, *Science* **351**, 1447 (2016).
- ¹⁴M. Bilde, K. Barsanti, M. Booth, C. D. Cappa, N. M. Donahue, E. U. Emanuelsson, G. McFiggans, U. K. Krieger, C. Marcolli, D. Topping, P. Ziemann, M. Barley, S. Clegg, B. Dennis-Smith, M. Hallquist, A. M. Hallquist, A. Khlystov, M. Kulmala, D. Mogens, C. J. Percival, F. Pope, J. P. Reid, M. da Silva, T. Rosenoern, K. Salo, V. P. Soonsin, T. Yli-Juuti, N. L. Prisle, J. Pagels, J. Rarey, A. A. Zardini, and I. Riipinen, *Chem. Rev.* **115**, 4115 (2015).

- ¹⁵B. R. Bzdek, J. W. DePalma, and M. V. Johnston, *Acc. Chem. Res.* **50**, 1965 (2017).
- ¹⁶J. Kirkby, J. Curtius, J. Almeida, E. Dunne, J. Duplissy, S. Ehrhart, A. Franchin, S. Gagne, L. Ickes, A. Kurten, A. Kupc, A. Metzger, F. Riccobono, L. Rondo, S. Schobesberger, G. Tsagkogeorgas, D. Wimmer, A. Amorim, F. Bianchi, M. Breitenlechner, A. David, J. Dommen, A. Downard, M. Ehn, R. C. Flagan, S. Haider, A. Hansel, D. Hauser, W. Jud, H. Junninen, F. Kreissl, A. Kvashin, A. Laaksonen, K. Lehtipalo, J. Lima, E. R. Lovejoy, V. Makhmutov, S. Mathot, J. Mikkila, P. Minginette, S. Mogo, T. Nieminen, A. Onnela, P. Pereira, T. Petaja, R. Schnitzhofer, J. H. Seinfeld, M. Sipila, Y. Stozhkov, F. Stratmann, A. Tome, J. Vanhanen, Y. Viisanen, A. Virtala, P. E. Wagner, H. Walther, E. Weingartner, H. Wex, P. M. Winkler, K. S. Carslaw, D. R. Worsnop, U. Baltensperger, and M. Kulmala, *Nature* **476**, 429 (2011).
- ¹⁷C. N. Jen, P. H. McMurry, and D. R. Hanson, *J. Geophys. Res.: Atmos.* **119**, 7502, <https://doi.org/10.1002/2014jd021592> (2014).
- ¹⁸T. Olenius, O. Kupiainen-Maatta, I. K. Ortega, T. Kurten, and H. Vehkamaki, *J. Chem. Phys.* **139**, 084312 (2013).
- ¹⁹S. Chakrabarty, J. J. Ferreiro, M. Lippe, and R. Signorell, *J. Phys. Chem. A* **121**, 3991 (2017).
- ²⁰J. J. Ferreiro, S. Chakrabarty, B. Schlappi, and R. Signorell, *J. Chem. Phys.* **145**, 211907 (2016).
- ²¹Y. Park, S. Tanimura, and B. E. Wyslouzil, *Aerosol Sci. Technol.* **50**, 773 (2016).
- ²²H. Pathak, K. Mullick, S. Tanimura, and B. E. Wyslouzil, *Aerosol Sci. Technol.* **47**, 1310 (2013).
- ²³H. Pathak, J. Wolk, R. Strey, and B. E. Wyslouzil, *J. Chem. Phys.* **140**, 034304 (2014).
- ²⁴P. Davidovits, C. E. Kolb, L. R. Williams, J. T. Jayne, and D. R. Worsnop, *Chem. Rev.* **111**, PR76 (2011).
- ²⁵C. E. Kolb, R. A. Cox, J. P. D. Abbatt, M. Ammann, E. J. Davis, D. J. Donaldson, B. C. Garrett, C. George, P. T. Griffiths, D. R. Hanson, M. Kulmala, G. McFiggans, U. Poschl, I. Riipinen, M. J. Rossi, Y. Rudich, P. E. Wagner, P. M. Winkler, D. R. Worsnop, and C. D. O'Dowd, *Atmos. Chem. Phys.* **10**, 10561 (2010).
- ²⁶H. Vehkamaki and I. Riipinen, *Chem. Soc. Rev.* **41**, 5160 (2012).
- ²⁷G. M. Nathanson, *Annu. Rev. Phys. Chem.* **55**, 231 (2004).
- ²⁸P. Jungwirth and B. Winter, *Annu. Rev. Phys. Chem.* **59**, 343 (2008).
- ²⁹W. G. Li and E. J. Davis, *Aerosol Sci. Technol.* **25**, 11 (1996).
- ³⁰A. H. Persad and C. A. Ward, *Chem. Rev.* **116**, 7727 (2016).
- ³¹E. J. Davis and G. Schweiger, *The Airborne Microparticle: Its Physics, Chemistry, Optics, and Transport Phenomena* (Springer-Verlag, Berlin, Germany, 2002).
- ³²J. F. Davies, R. E. H. Miles, A. E. Haddrell, and J. P. Reid, *Proc. Natl. Acad. Sci. U. S. A.* **110**, 8807 (2013).
- ³³R. M. Power and J. P. Reid, *Rep. Prog. Phys.* **77**, 074601 (2014).
- ³⁴B. R. Bzdek, L. Collard, J. E. Sprittles, A. J. Hudson, and J. P. Reid, *J. Chem. Phys.* **145**, 054502 (2016).
- ³⁵B. R. Bzdek, R. M. Power, S. H. Simpson, J. P. Reid, and C. P. Royall, *Chem. Sci.* **7**, 274 (2016).
- ³⁶K. Ardon-Dryer, Y. W. Huang, and D. J. Cziczo, *Atmos. Chem. Phys.* **15**, 9159 (2015).
- ³⁷F. Y. Testik and M. K. Rahman, *Geophys. Res. Lett.* **44**, 1175, <https://doi.org/10.1002/2017gl072516> (2017).
- ³⁸R. M. Power, D. R. Burnham, and J. P. Reid, *Appl. Opt.* **53**, 8522 (2014).
- ³⁹E. Bichoutskaia, A. L. Boatwright, A. Khachatourian, and A. J. Stace, *J. Chem. Phys.* **133**, 024105 (2010).
- ⁴⁰E. B. Lindgren, H. K. Chan, A. J. Stace, and E. Besley, *Phys. Chem. Chem. Phys.* **18**, 5883 (2016).
- ⁴¹J. Kohno, T. Higashiura, T. Eguchi, S. Miura, and M. Ogawa, *J. Phys. Chem. B* **120**, 7696 (2016).
- ⁴²T. Suzuki and J. Y. Kohno, *J. Phys. Chem. B* **118**, 5781 (2014).
- ⁴³R. Power, J. P. Reid, S. Anand, D. McGloin, A. Almohamedi, N. S. Mistry, and A. J. Hudson, *J. Phys. Chem. A* **116**, 8873 (2012).
- ⁴⁴R. D. Davis, S. Lance, J. A. Gordon, and M. A. Tolbert, *Anal. Chem.* **87**, 6186 (2015).
- ⁴⁵R. D. Davis and M. A. Tolbert, *Sci. Adv.* **3**, e1700425 (2017).
- ⁴⁶R. D. Davis, S. Lance, J. A. Gordon, S. B. Ushijima, and M. A. Tolbert, *Proc. Natl. Acad. Sci. U. S. A.* **112**, 15815 (2015).
- ⁴⁷T. Koop, J. Bookhold, M. Shiraiwa, and U. Poeschl, *Phys. Chem. Chem. Phys.* **13**, 19238 (2011).
- ⁴⁸E. Mikhailov, S. Vlasenko, S. T. Martin, T. Koop, and U. Poeschl, *Atmos. Chem. Phys.* **9**, 9491 (2009).

- ⁴⁹A. Virtanen, J. Joutsensaari, T. Koop, J. Kannosto, P. Yli-Pirila, J. Leskinen, J. M. Makela, J. K. Holopainen, U. Poeschl, M. Kulmala, D. R. Worsnop, and A. Laaksonen, *Nature* **467**, 824 (2010).
- ⁵⁰B. Zobrist, C. Marcolli, D. A. Pedernera, and T. Koop, *Atmos. Chem. Phys.* **8**, 5221 (2008).
- ⁵¹E. Amstad, M. Gopinadhan, C. Holtze, C. O. Osuji, M. P. Brenner, F. Spaepen, and D. A. Weitz, *Science* **349**, 956 (2015).
- ⁵²S. Lee, H. S. Wi, W. Jo, Y. C. Cho, H. H. Lee, S. Y. Jeong, Y. I. Kim, and G. W. Lee, *Proc. Natl. Acad. Sci. U. S. A.* **113**, 13618 (2016).
- ⁵³M. Shiraiwa, Y. Li, A. P. Tsimpidi, V. A. Karydis, T. Berkemeier, S. N. Pandis, J. Lelieveld, T. Koop, and U. Pöschl, *Nat. Commun.* **8**, 15002 (2017).
- ⁵⁴M. Shiraiwa and J. H. Seinfeld, *Geophys. Res. Lett.* **39**, L24801, <https://doi.org/10.1029/2012gl016408> (2012).
- ⁵⁵B. B. Wang, T. H. Harder, S. T. Kelly, D. S. Pien, S. China, L. Kovarik, M. Keiluweit, B. W. Arey, M. K. Gilles, and A. Laskin, *Nat. Geosci.* **9**, 433 (2016).
- ⁵⁶Q. Ye, E. S. Robinson, X. Ding, P. Ye, R. C. Sullivan, and N. M. Donahue, *Proc. Natl. Acad. Sci. U. S. A.* **113**, 12649 (2016).
- ⁵⁷A. Athanasiadis, C. Fitzgerald, N. M. Davidson, C. Giorio, S. W. Botchway, A. D. Ward, M. Kalberer, F. D. Pope, and M. K. Kuimova, *Phys. Chem. Chem. Phys.* **18**, 30385 (2016).
- ⁵⁸F. H. Marshall, R. E. H. Miles, Y. C. Song, P. B. Ohm, R. M. Power, J. P. Reid, and C. S. Dutcher, *Chem. Sci.* **7**, 1298 (2016).
- ⁵⁹M. Shiraiwa, M. Ammann, T. Koop, and U. Pöschl, *Proc. Natl. Acad. Sci. U. S. A.* **108**, 11003 (2011).
- ⁶⁰J. H. Slade and D. A. Knopf, *Geophys. Res. Lett.* **41**, 5297, <https://doi.org/10.1002/2014gl0106582> (2014).
- ⁶¹E. Abramson, D. Imre, J. Beranek, J. Wilson, and A. Zelenyuk, *Phys. Chem. Chem. Phys.* **15**, 2983 (2013).
- ⁶²V. Perraud, E. A. Bruns, M. J. Ezell, S. N. Johnson, Y. Yu, M. L. Alexander, A. Zelenyuk, D. Imre, W. L. Chang, D. Dabdub, J. F. Pankow, and B. J. Finlayson-Pitts, *Proc. Natl. Acad. Sci. U. S. A.* **109**, 2836 (2012).
- ⁶³M. Shrivastava, S. Lou, A. Zelenyuk, R. C. Easter, R. A. Corley, B. D. Thrall, P. J. Rasch, J. D. Fast, S. L. M. Simonich, H. Z. Shen, and S. Tao, *Proc. Natl. Acad. Sci. U. S. A.* **114**, 1246 (2017).
- ⁶⁴B. R. Bzdek and M. V. Johnston, *Anal. Chem.* **82**, 7871 (2010).
- ⁶⁵R. Y. Zhang, A. Khalizov, L. Wang, M. Hu, and W. Xu, *Chem. Rev.* **112**, 1957 (2012).
- ⁶⁶M. Kulmala, J. Kontkanen, H. Junninen, K. Lehtipalo, H. E. Manninen, T. Nieminen, T. Petaja, M. Sipila, S. Schobesberger, P. Rantala, A. Franchin, T. Jokinen, E. Jarvinen, M. Aijala, J. Kangasluoma, J. Hakala, P. P. Aalto, P. Paasonen, J. Mikkila, J. Vanhanen, J. Aalto, H. Hakola, U. Makkonen, T. Ruuskanen, R. L. Mauldin, J. Duplissy, H. Vehkamäki, J. Back, A. Kortelainen, I. Riipinen, T. Kurten, M. V. Johnston, J. N. Smith, M. Ehn, T. F. Mentel, K. E. J. Lehtinen, A. Laaksonen, V. M. Kerminen, and D. R. Worsnop, *Science* **339**, 943 (2013).
- ⁶⁷C. Kuang, P. H. McMurry, A. V. McCormick, and F. L. Eisele, *J. Geophys. Res.: Atmos.* **113**, D10209, <https://doi.org/10.1029/2007jd009253> (2008).
- ⁶⁸F. Bianchi, J. Trostl, H. Junninen, C. Frege, S. Henne, C. R. Hoyle, U. Molteni, E. Herrmann, A. Adamov, N. Bukowiecki, X. Chen, J. Duplissy, M. Gysel, M. Hutterli, J. Kangasluoma, J. Kontkanen, A. Kurten, H. E. Manninen, S. Munch, O. Perakyla, T. Petaja, L. Rondo, C. Williamson, E. Weingartner, J. Curtius, D. R. Worsnop, M. Kulmala, J. Dommen, and U. Baltensperger, *Science* **352**, 1109 (2016).
- ⁶⁹J. Merikanto, D. V. Spracklen, G. W. Mann, S. J. Pickering, and K. S. Carslaw, *Atmos. Chem. Phys.* **9**, 8601 (2009).
- ⁷⁰U. Lohmann and J. Feichter, *Atmos. Chem. Phys.* **5**, 715 (2005).
- ⁷¹B. E. Wyslouzil and J. Wolk, *J. Chem. Phys.* **145**, 211702 (2016).
- ⁷²M. Kulmala, I. Riipinen, M. Sipila, H. E. Manninen, T. Petaja, H. Junninen, M. Dal Maso, G. Mordas, A. Mirme, M. Vana, A. Hirsikko, L. Laakso, R. M. Harrison, I. Hanson, C. Leung, K. E. J. Lehtinen, and V. M. Kerminen, *Science* **318**, 89 (2007).
- ⁷³M. Kulmala, H. Vehkamäki, T. Petäjä, M. Dal Maso, A. Lauri, V. M. Kerminen, W. Birmili, and P. H. McMurry, *J. Aerosol Sci.* **35**, 143 (2004).
- ⁷⁴H. Vehkamäki, M. J. McGrath, T. Kurten, J. Julin, K. E. J. Lehtinen, and M. Kulmala, *J. Chem. Phys.* **136**, 094107 (2012).
- ⁷⁵C. Kuang, M. Chen, J. Zhao, J. Smith, P. H. McMurry, and J. Wang, *Atmos. Chem. Phys.* **12**, 3573 (2012).
- ⁷⁶C. Kuang, I. Riipinen, S. L. Sihto, M. Kulmala, A. V. McCormick, and P. H. McMurry, *Atmos. Chem. Phys.* **10**, 8469 (2010).
- ⁷⁷M. R. Stolzenburg, P. H. McMurry, H. Sakurai, J. N. Smith, R. L. Mauldin, F. L. Eisele, and C. F. Clement, *J. Geophys. Res.: Atmos.* **110**, D22S05, <https://doi.org/10.1029/2005jd005935> (2005).
- ⁷⁸J. Zhao, J. N. Smith, F. L. Eisele, M. Chen, C. Kuang, and P. H. McMurry, *Atmos. Chem. Phys.* **11**, 10823 (2011).
- ⁷⁹J. N. Smith, K. C. Barsanti, H. R. Friedli, M. Ehn, M. Kulmala, D. R. Collins, J. H. Scheckman, B. J. Williams, and P. H. McMurry, *Proc. Natl. Acad. Sci. U. S. A.* **107**, 6634 (2010).
- ⁸⁰J. Almeida, S. Schobesberger, A. Kurten, I. K. Ortega, O. Kupiainen-Maatta, A. P. Praplan, A. Adamov, A. Amorim, F. Bianchi, M. Breitenlechner, A. David, J. Dommen, N. M. Donahue, A. Downard, E. Dunne, J. Duplissy, S. Ehrhart, R. C. Flagan, A. Franchin, R. Guida, J. Hakala, A. Hansel, M. Heinritzi, H. Henschel, T. Jokinen, H. Junninen, M. Kajos, J. Kangasluoma, H. Keskinen, A. Kupc, T. Kurten, A. N. Kvashin, A. Laaksonen, K. Lehtipalo, M. Leiminger, J. Leppa, V. Loukonen, V. Makhmutov, S. Mathot, M. J. McGrath, T. Nieminen, T. Olenin, A. Onnela, T. Petaja, F. Riccobono, I. Riipinen, M. Rissanen, L. Rondo, T. Ruuskanen, F. D. Santos, N. Sarnela, S. Schallhart, R. Schnitzhofer, J. H. Seinfeld, M. Simon, M. Sipila, Y. Stozhkov, F. Stratmann, A. Tome, J. Trostl, G. Tsagkogeorgas, P. Vaattovaara, Y. Viisanen, A. Virtanen, A. Virtala, P. E. Wagner, E. Weingartner, H. Wex, C. Williamson, D. Wimmer, P. L. Ye, T. Yli-Juuti, K. S. Carslaw, M. Kulmala, J. Curtius, U. Baltensperger, D. R. Worsnop, H. Vehkamäki, and J. Kirkby, *Nature* **502**, 359 (2013).
- ⁸¹A. Kurten, T. Jokinen, M. Simon, M. Sipila, N. Sarnela, H. Junninen, A. Adamov, J. Almeida, A. Amorim, F. Bianchi, M. Breitenlechner, J. Dommen, N. M. Donahue, J. Duplissy, S. Ehrhart, R. C. Flagan, A. Franchin, J. Hakala, A. Hansel, M. Heinritzi, M. Hutterli, J. Kangasluoma, J. Kirkby, A. Laaksonen, K. Lehtipalo, M. Leiminger, V. Makhmutov, S. Mathot, A. Onnela, T. Petaja, A. P. Praplan, F. Riccobono, M. P. Rissanen, L. Rondo, S. Schobesberger, J. H. Seinfeld, G. Steiner, A. Tome, J. Trostl, P. M. Winkler, C. Williamson, D. Wimmer, P. L. Ye, U. Baltensperger, K. S. Carslaw, M. Kulmala, D. R. Worsnop, and J. Curtius, *Proc. Natl. Acad. Sci. U. S. A.* **111**, 15019 (2014).
- ⁸²A. Kürten, C. Li, F. Bianchi, J. Curtius, A. Dias, N. M. Donahue, J. Duplissy, R. C. Flagan, J. Hakala, T. Jokinen, J. Kirkby, M. Kulmala, A. Laaksonen, K. Lehtipalo, V. Makhmutov, A. Onnela, M. P. Rissanen, M. Simon, M. Sipilä, Y. Stozhkov, J. Tröstl, P. Ye, and P. H. McMurry, "New particle formation in the sulfuric acid-dimethylamine-water system: Reevaluation of CLOUD chamber measurements and comparison to an aerosol nucleation and growth model," *Atmos. Chem. Phys.* (to be published).
- ⁸³B. R. Bzdek, J. W. DePalma, D. P. Ridge, J. Laskin, and M. V. Johnston, *J. Am. Chem. Soc.* **135**, 3276 (2013).
- ⁸⁴B. R. Bzdek, D. P. Ridge, and M. V. Johnston, *Atmos. Chem. Phys.* **11**, 8735 (2011).
- ⁸⁵J. W. DePalma, B. R. Bzdek, D. J. Doren, and M. V. Johnston, *J. Phys. Chem. A* **116**, 1030 (2012).
- ⁸⁶C. J. Johnson and M. A. Johnson, *J. Phys. Chem. A* **117**, 13265 (2013).
- ⁸⁷B. R. Bzdek, D. P. Ridge, and M. V. Johnston, *J. Phys. Chem. A* **114**, 11638 (2010).
- ⁸⁸B. R. Bzdek, D. P. Ridge, and M. V. Johnston, *Atmos. Chem. Phys.* **10**, 3495 (2010).
- ⁸⁹B. R. Bzdek, D. P. Ridge, and M. V. Johnston, *J. Geophys. Res.: Atmos.* **116**, D03301, <https://doi.org/10.1029/2010jd015217> (2011).
- ⁹⁰K. C. Barsanti, J. H. Kroll, and J. A. Thornton, *J. Phys. Chem. Lett.* **8**, 1503 (2017).
- ⁹¹P. M. Winkler, J. Ortega, T. Karl, L. Cappellin, H. R. Friedli, K. Barsanti, P. H. McMurry, and J. N. Smith, *Geophys. Res. Lett.* **39**, L20815, <https://doi.org/10.1029/2012gl0163253> (2012).
- ⁹²J. Zhao, J. Ortega, M. Chen, P. H. McMurry, and J. N. Smith, *Atmos. Chem. Phys.* **13**, 7631 (2013).
- ⁹³R. Y. Zhang, I. Suh, J. Zhao, D. Zhang, E. C. Fortner, X. X. Tie, L. T. Molina, and M. J. Molina, *Science* **304**, 1487 (2004).
- ⁹⁴J. Kirkby, J. Duplissy, K. Sengupta, C. Frege, H. Gordon, C. Williamson, M. Heinritzi, M. Simon, C. Yan, J. Almeida, J. Trostl, T. Nieminen, I. K. Ortega, R. Wagner, A. Adamov, A. Amorim, A. K. Bernhammer, F. Bianchi, M. Breitenlechner, S. Brilke, X. M. Chen, J. Craven, A. Dias, S. Ehrhart, R. C. Flagan, A. Franchin, C. Fuchs, R. Guida, J. Hakala, C. R. Hoyle, T. Jokinen, H. Junninen, J. Kangasluoma, J. Kim, M. Krapf, A. Kurten, A. Laaksonen, K. Lehtipalo, V. Makhmutov, S. Mathot, U. Molteni, A. Onnela, O. Perakyla, F. Piel, T. Petaja, A. P. Praplan, K. Pringle, A. Rap, N. A. D. Richards, I. Riipinen, M. P. Rissanen, L. Rondo,

- N. Sarnela, S. Schobesberger, C. E. Scott, J. H. Seinfeld, M. Sipila, G. Steiner, Y. Stozhkov, F. Stratmann, A. Tome, A. Virtanen, A. L. Vogel, A. C. Wagner, P. E. Wagner, E. Weingartner, D. Wimmer, P. M. Winkler, P. L. Ye, X. Zhang, A. Hansel, J. Dommen, N. M. Donahue, D. R. Worsnop, U. Baltensperger, M. Kulmala, K. S. Carslaw, and J. Curtius, *Nature* **533**, 521 (2016).
- ⁹⁵M. Ehn, J. A. Thornton, E. Kleist, M. Sipila, H. Junninen, I. Pullinen, M. Springer, F. Rubach, R. Tillmann, B. Lee, F. Lopez-Hilfiker, S. Andres, I. H. Acir, M. Rissanen, T. Jokinen, S. Schobesberger, J. Kangasluoma, J. Kontkanen, T. Nieminen, T. Kurten, L. B. Nielsen, S. Jorgensen, H. G. Kjaergaard, M. Canagaratna, M. Dal Maso, T. Berndt, T. Petaja, A. Wahner, V. M. Kerminen, M. Kulmala, D. R. Worsnop, J. Wildt, and T. F. Mentel, *Nature* **506**, 476 (2014).
- ⁹⁶F. Riccobono, S. Schobesberger, C. E. Scott, J. Dommen, I. K. Ortega, L. Rondo, J. Almeida, A. Amorim, F. Bianchi, M. Breitenlechner, A. David, A. Downard, E. M. Dunne, J. Duplissy, S. Ehrhart, R. C. Flagan, A. Franchin, A. Hansel, H. Junninen, M. Kajos, H. Keskinen, A. Kupc, A. Kurten, A. N. Kvashin, A. Laaksonen, K. Lehtipalo, V. Makhmutov, S. Mathot, T. Nieminen, A. Onnela, T. Petaja, A. P. Praplan, F. D. Santos, S. Schallhart, J. H. Seinfeld, M. Sipila, D. V. Spracklen, Y. Stozhkov, F. Stratmann, A. Tome, G. Tsagkogeorgas, P. Vaattovaara, Y. Viisanen, A. Vrtala, P. E. Wagner, E. Weingartner, H. Wex, D. Wimmer, K. S. Carslaw, J. Curtius, N. M. Donahue, J. Kirkby, M. Kulmala, D. R. Worsnop, and U. Baltensperger, *Science* **344**, 717 (2014).
- ⁹⁷S. Schobesberger, H. Junninen, F. Bianchi, G. Lonn, M. Ehn, K. Lehtipalo, J. Dommen, S. Ehrhart, I. K. Ortega, A. Franchin, T. Nieminen, F. Riccobono, M. Hutterli, J. Duplissy, J. Almeida, A. Amorim, M. Breitenlechner, A. J. Downard, E. M. Dunne, R. C. Flagan, M. Kajos, H. Keskinen, J. Kirkby, A. Kupc, A. Kurten, T. Kurten, A. Laaksonen, S. Mathot, A. Onnela, A. P. Praplan, L. Rondo, F. D. Santos, S. Schallhart, R. Schnitzhofer, M. Sipila, A. Tome, G. Tsagkogeorgas, H. Vehkamäki, D. Wimmer, U. Baltensperger, K. S. Carslaw, J. Curtius, A. Hansel, T. Petaja, M. Kulmala, N. M. Donahue, and D. R. Worsnop, *Proc. Natl. Acad. Sci. U. S. A.* **110**, 17223 (2013).
- ⁹⁸T. Jokinen, M. Sipila, S. Richters, V. M. Kerminen, P. Paasonen, F. Stratmann, D. Worsnop, M. Kulmala, M. Ehn, H. Herrmann, and T. Berndt, *Angew. Chem., Int. Ed.* **53**, 14596 (2014).
- ⁹⁹J. D. Crouse, L. B. Nielsen, S. Jorgensen, H. G. Kjaergaard, and P. O. Wennberg, *J. Phys. Chem. Lett.* **4**, 3513 (2013).
- ¹⁰⁰T. F. Mentel, M. Springer, M. Ehn, E. Kleist, I. Pullinen, T. Kurten, M. Rissanen, A. Wahner, and J. Wildt, *Atmos. Chem. Phys.* **15**, 6745 (2015).
- ¹⁰¹M. P. Rissanen, T. Kurten, M. Sipila, J. A. Thornton, J. Kangasluoma, N. Sarnela, H. Junninen, S. Jorgensen, S. Schallhart, M. K. Kajos, R. Taipale, M. Springer, T. F. Mentel, T. Ruuskanen, T. Petaja, D. R. Worsnop, H. G. Kjaergaard, and M. Ehn, *J. Am. Chem. Soc.* **136**, 15596 (2014).
- ¹⁰²K. J. Heaton, M. A. Dreyfus, S. Wang, and M. V. Johnston, *Environ. Sci. Technol.* **41**, 6129 (2007).
- ¹⁰³J. D. Savee, E. Papajak, B. Rotavera, H. F. Huang, A. J. Eskola, O. Welz, L. Sheps, C. A. Taatjes, J. Zador, and D. L. Osborn, *Science* **347**, 643 (2015).
- ¹⁰⁴J. Zador, H. F. Huang, O. Welz, J. Zetterberg, D. L. Osborn, and C. A. Taatjes, *Phys. Chem. Chem. Phys.* **15**, 10753 (2013).
- ¹⁰⁵J. Trostl, W. K. Chuang, H. Gordon, M. Heinritzi, C. Yan, U. Molteni, L. Ahlm, C. Frege, F. Bianchi, R. Wagner, M. Simon, K. Lehtipalo, C. Williamson, J. S. Craven, J. Duplissy, A. Adamov, J. Almeida, A. K. Bernhammer, M. Breitenlechner, S. Brilke, A. Dias, S. Ehrhart, R. C. Flagan, A. Franchin, C. Fuchs, R. Guida, M. Gysel, A. Hansel, C. R. Hoyle, T. Jokinen, H. Junninen, J. Kangasluoma, H. Keskinen, J. Kim, M. Krapf, A. Kurten, A. Laaksonen, M. Lawler, M. Leiminger, S. Mathot, O. Mohler, T. Nieminen, A. Onnela, T. Petaja, F. M. Piel, P. Miettinen, M. P. Rissanen, L. Rondo, N. Sarnela, S. Schobesberger, K. Sengupta, M. Sipila, J. N. Smith, G. Steiner, A. Tome, A. Virtanen, A. C. Wagner, E. Weingartner, D. Wimmer, P. M. Winkler, P. L. Ye, K. S. Carslaw, J. Curtius, J. Dommen, J. Kirkby, M. Kulmala, I. Riipinen, D. R. Worsnop, N. M. Donahue, and U. Baltensperger, *Nature* **533**, 527 (2016).
- ¹⁰⁶T. Kurten, K. Tiusanen, P. Roldin, M. Rissanen, J. N. Luy, M. Boy, M. Ehn, and N. M. Donahue, *J. Phys. Chem. A* **120**, 2569 (2016).
- ¹⁰⁷J. Wang and A. S. Wexler, *Geophys. Res. Lett.* **40**, 2834, <https://doi.org/10.1002/grl.50455> (2013).
- ¹⁰⁸M. J. Apsokardu and M. V. Johnston, "Nanoparticle growth by particle phase chemistry," *Atmos. Chem. Phys.* (to be published).
- ¹⁰⁹M. Shiraiwa, L. D. Yee, K. A. Schilling, C. L. Loza, J. S. Craven, A. Zuend, P. J. Ziemann, and J. H. Seinfeld, *Proc. Natl. Acad. Sci. U. S. A.* **110**, 11746 (2013).
- ¹¹⁰P. Tu and M. V. Johnston, *Atmos. Chem. Phys.* **17**, 7593 (2017).
- ¹¹¹Y. Wu and M. V. Johnston, *Environ. Sci. Technol.* **51**, 4445 (2017).
- ¹¹²R. Zhao, D. Aljawhary, A. K. Y. Lee, and J. P. D. Abbatt, *Environ. Sci. Technol. Lett.* **4**, 205 (2017).
- ¹¹³A. P. Bateman, S. A. Nizkorodov, J. Laskin, and A. Laskin, *Phys. Chem. Chem. Phys.* **13**, 12199 (2011).
- ¹¹⁴J. Ovadnevaite, A. Zuend, A. Laaksonen, K. J. Sanchez, G. Roberts, D. Ceburnis, S. Decesari, M. Rinaldi, N. Hodas, M. C. Facchini, J. H. Seinfeld, and C. O' Dowd, *Nature* **546**, 637 (2017).
- ¹¹⁵D. M. Cwiertny, M. A. Young, and V. H. Grassian, *Annu. Rev. Phys. Chem.* **59**, 27 (2008).
- ¹¹⁶C. R. Usher, A. E. Michel, and V. H. Grassian, *Chem. Rev.* **103**, 4883 (2003).
- ¹¹⁷D. Lowe and A. R. MacKenzie, *J. Atmos. Sol.-Terr. Phys.* **70**, 13 (2008).
- ¹¹⁸G. Rubasinghege, S. Elzey, J. Baltrusaitis, P. M. Jayaweera, and V. H. Grassian, *J. Phys. Chem. Lett.* **1**, 1729 (2010).
- ¹¹⁹J. Schuttlefield, G. Rubasinghege, M. El-Maazawi, J. Bone, and V. H. Grassian, *J. Am. Chem. Soc.* **130**, 12210 (2008).
- ¹²⁰M. J. Molina, T. L. Tso, L. T. Molina, and F. C. Y. Wang, *Science* **238**, 1253 (1987).
- ¹²¹E. M. Knipping, M. J. Lakin, K. L. Foster, P. Jungwirth, D. J. Tobias, R. B. Gerber, D. Dabdub, and B. J. Finlayson-Pitts, *Science* **288**, 301 (2000).
- ¹²²T. Berkemeier, S. S. Steimer, U. K. Krieger, T. Peter, U. Poschl, M. Ammann, and M. Shiraiwa, *Phys. Chem. Chem. Phys.* **18**, 12662 (2016).
- ¹²³C. J. Gaston and J. A. Thornton, *J. Phys. Chem. A* **120**, 1039 (2016).
- ¹²⁴D. R. Hanson and A. R. Ravishankara, *J. Phys. Chem.* **98**, 5728 (1994).
- ¹²⁵S. F. Maria, L. M. Russell, M. K. Gilles, and S. C. B. Myneni, *Science* **306**, 1921 (2004).
- ¹²⁶A. M. Jubb, W. Hua, and H. C. Allen, *Acc. Chem. Res.* **45**, 110 (2012).
- ¹²⁷S. N. Wren, B. P. Gordon, N. A. Valley, L. E. McWilliams, and G. L. Richmond, *J. Phys. Chem. A* **119**, 6391 (2015).
- ¹²⁸S. Gopalakrishnan, D. F. Liu, H. C. Allen, M. Kuo, and M. J. Shultz, *Chem. Rev.* **106**, 1155 (2006).
- ¹²⁹S. G. Moussa, T. M. McIntire, M. Szori, M. Roeselova, D. J. Tobias, R. L. Grimm, J. C. Hemminger, and B. J. Finlayson-Pitts, *J. Phys. Chem. A* **113**, 2060 (2009).
- ¹³⁰J. C. Hemminger, *Int. Rev. Phys. Chem.* **18**, 387 (1999).
- ¹³¹M. Shrestha, Y. Zhang, M. A. Upshur, P. Liu, S. L. Blair, H.-F. Wang, S. A. Nizkorodov, R. J. Thomson, S. T. Martin, and F. M. Geiger, *J. Phys. Chem. A* **119**, 4609 (2015).
- ¹³²U. K. Krieger, M. Hess, T. Peter, A. Rossi, N. D. Spencer, and W. A. Lanford, *Phys. Rev. Lett.* **111**, 266102 (2013).
- ¹³³K. Nakajima, A. Ohno, M. Suzuki, and K. Kimura, *Nucl. Instrum. Methods Phys. Res., Sect. B* **267**, 605 (2009).
- ¹³⁴M. Tassotto, T. J. Gannon, and P. R. Watson, *J. Chem. Phys.* **107**, 8899 (1997).
- ¹³⁵S. Ghosal, J. C. Hemminger, H. Bluhm, B. S. Mun, E. L. D. Hebenstreit, G. Ketteler, D. F. Ogletree, F. G. Requejo, and M. Salmeron, *Science* **307**, 563 (2005).
- ¹³⁶R. E. H. Miles, J. F. Davies, and J. P. Reid, *Phys. Chem. Chem. Phys.* **18**, 19847 (2016).
- ¹³⁷D. O. Topping, G. B. McFiggans, G. Kiss, Z. Varga, M. C. Facchini, S. Decesari, and M. Mircea, *Atmos. Chem. Phys.* **7**, 2371 (2007).
- ¹³⁸H. Wex, F. Stratmann, D. Topping, and G. McFiggans, *J. Atmos. Sci.* **65**, 4004 (2008).
- ¹³⁹C. R. Ruehl, P. Y. Chuang, A. Nenes, C. D. Cappa, K. R. Kolesar, and A. H. Goldstein, *Geophys. Res. Lett.* **39**, L23801, <https://doi.org/10.1029/2012gl053706> (2012).
- ¹⁴⁰C. R. Ruehl and K. R. Wilson, *J. Phys. Chem. A* **118**, 3952 (2014).
- ¹⁴¹E. R. Mysak, D. E. Starr, K. R. Wilson, and H. Bluhm, *Rev. Sci. Instrum.* **81**, 016106 (2010).
- ¹⁴²D. E. Starr, E. K. Wong, D. R. Worsnop, K. R. Wilson, and H. Bluhm, *Phys. Chem. Chem. Phys.* **10**, 3093 (2008).
- ¹⁴³M. I. Jacobs, B. Xu, O. Kostko, N. Heine, M. Ahmed, and K. R. Wilson, *J. Phys. Chem. A* **120**, 8645 (2016).
- ¹⁴⁴Y. Wu, W. Li, B. Xu, X. Li, H. Wang, V. F. McNeill, Y. Rao, and H.-L. Dai, *J. Phys. Chem. Lett.* **7**, 2294 (2016).
- ¹⁴⁵H. S. Morris, V. H. Grassian, and A. V. Tivanski, *Chem. Sci.* **6**, 3242 (2015).
- ¹⁴⁶H. C. Boyer and C. S. Dutcher, *J. Phys. Chem. A* **121**, 4733 (2017).

- ¹⁴⁷H. C. Boyer, B. R. Bzdek, J. P. Reid, and C. S. Dutcher, *J. Phys. Chem. A* **121**, 198 (2017).
- ¹⁴⁸B. Noziere, C. Baduel, and J.-L. Jaffrezo, *Nat. Commun.* **5**, 3335 (2014).
- ¹⁴⁹R. Sorjamaa, B. Svenningsson, T. Raatikainen, S. Henning, M. Bilde, and A. Laaksonen, *Atmos. Chem. Phys.* **4**, 2107 (2004).
- ¹⁵⁰S. Lowe, D. G. Partridge, D. Topping, and P. Stier, *Atmos. Chem. Phys.* **16**, 10941 (2016).
- ¹⁵¹N. L. Prisle, A. Asmi, D. Topping, A. I. Partanen, S. Romakkaniemi, M. Dal Maso, M. Kulmala, A. Laaksonen, K. E. J. Lehtinen, G. McFiggans, and H. Kokkola, *Geophys. Res. Lett.* **39**, L05802, <https://doi.org/10.1029/2011gl050467> (2012).
- ¹⁵²T. Raatikainen and A. Laaksonen, *Geosci. Model Dev.* **4**, 107 (2011).
- ¹⁵³D. Topping, *Geosci. Model Dev.* **3**, 635 (2010).
- ¹⁵⁴C. Cai, D. J. Stewart, T. C. Preston, J. S. Walker, Y. H. Zhang, and J. P. Reid, *Phys. Chem. Chem. Phys.* **16**, 3162 (2014).
- ¹⁵⁵C. Cai, D. J. Stewart, J. P. Reid, Y. H. Zhang, P. Ohm, C. S. Dutcher, and S. L. Clegg, *J. Phys. Chem. A* **119**, 704 (2015).
- ¹⁵⁶T. C. Preston and J. P. Reid, *J. Opt. Soc. Am. A* **32**, 2210 (2015).
- ¹⁵⁷S. Bastelberger, U. K. Krieger, B. P. Luo, and T. Peter, *Atmos. Chem. Phys.* **17**, 8453 (2017).
- ¹⁵⁸A. Baldelli, R. M. Power, R. E. H. Miles, J. P. Reid, and R. Vehring, *Aerosol Sci. Technol.* **50**, 693 (2016).
- ¹⁵⁹I. N. Tang and H. R. Munkelwitz, *Aerosol Sci. Technol.* **15**, 201 (1991).
- ¹⁶⁰G. Hargreaves, N. O. A. Kwamena, Y. H. Zhang, J. R. Butler, S. Rushworth, S. L. Clegg, and J. P. Reid, *J. Phys. Chem. A* **114**, 1806 (2010).
- ¹⁶¹G. Rovelli, R. E. H. Miles, J. P. Reid, and S. L. Clegg, *J. Phys. Chem. A* **120**, 4376 (2016).
- ¹⁶²A. Marsh, G. Rovelli, Y.-C. Song, K. L. Pereira, R. E. Willoughby, B. R. Bzdek, J. F. Hamilton, A. J. Orr-Ewing, D. O. Topping, and J. P. Reid, *Faraday Discuss.* **200**, 639 (2017).
- ¹⁶³N. Rastak, A. Pajunoja, J. C. A. Navarro, J. Ma, M. Song, D. G. Partridge, A. Kirkevåg, Y. Leong, W. W. Hu, N. F. Taylor, A. Lambe, K. Cerully, A. Bougiatioti, P. Liu, R. Krejci, T. Petaja, C. Percival, P. Davidovits, D. R. Worsnop, A. M. L. Ekman, A. Nenes, S. Martin, J. L. Jimenez, D. R. Collins, D. O. Topping, A. K. Bertram, A. Zuend, A. Virtanen, and I. Riipinen, *Geophys. Res. Lett.* **44**, 5167, <https://doi.org/10.1002/2017gl073056> (2017).
- ¹⁶⁴A. E. Haddrell, J. F. Davies, R. E. H. Miles, J. P. Reid, L. A. Dailey, and D. Murnane, *Int. J. Pharm.* **463**, 50 (2014).
- ¹⁶⁵A. Pajunoja, A. T. Lambe, J. Hakala, N. Rastak, M. J. Cummings, J. F. Brogan, L. Q. Hao, M. Paramonov, J. Hong, N. L. Prisle, J. Malila, S. Romakkaniemi, K. E. J. Lehtinen, A. Laaksonen, M. Kulmala, P. Massoli, T. B. Onasch, N. M. Donahue, I. Riipinen, P. Davidovits, D. R. Worsnop, T. Petaja, and A. Virtanen, *Geophys. Res. Lett.* **42**, 3063, <https://doi.org/10.1002/2015gl063142> (2015).
- ¹⁶⁶D. M. Broday and P. G. Georgopoulos, *Aerosol Sci. Technol.* **34**, 144 (2001).
- ¹⁶⁷L. Golshahi, G. Tian, M. Azimi, Y. J. Son, R. Walenga, P. W. Longest, and M. Hindle, *Pharm. Res.* **30**, 2917 (2013).
- ¹⁶⁸N. Grasmeijer, H. W. Frijlink, and W. L. J. Hinrichs, *J. Aerosol Sci.* **93**, 21 (2016).
- ¹⁶⁹G. Tian, P. W. Longest, X. Li, and M. Hindle, *J. Aerosol Med. Pulm. Drug Delivery* **26**, 248 (2013).
- ¹⁷⁰J. L. Jimenez, M. R. Canagaratna, N. M. Donahue, A. S. H. Prevot, Q. Zhang, J. H. Kroll, P. F. DeCarlo, J. D. Allan, H. Coe, N. L. Ng, A. C. Aiken, K. S. Docherty, I. M. Ulbrich, A. P. Grieshop, A. L. Robinson, J. Duplissy, J. D. Smith, K. R. Wilson, V. A. Lanz, C. Hueglin, Y. L. Sun, J. Tian, A. Laaksonen, T. Raatikainen, J. Rautiainen, P. Vaattovaara, M. Ehn, M. Kulmala, J. M. Tomlinson, D. R. Collins, M. J. Cubison, E. J. Dunlea, J. A. Huffman, T. B. Onasch, M. R. Alfarra, P. I. Williams, K. Bower, Y. Kondo, J. Schneider, F. Drewnick, S. Borrmann, S. Weimer, K. Demerjian, D. Salcedo, L. Cottrell, R. Griffin, A. Takami, T. Miyoshi, S. Hatakeyama, A. Shimono, J. Y. Sun, Y. M. Zhang, K. Dzepina, J. R. Kimmel, D. Sueper, J. T. Jayne, S. C. Herndon, A. M. Trimborn, L. R. Williams, E. C. Wood, A. M. Middlebrook, C. E. Kolb, U. Baltensperger, and D. R. Worsnop, *Science* **326**, 1525 (2009).
- ¹⁷¹Y. Li, U. Poschl, and M. Shiraiwa, *Atmos. Chem. Phys.* **16**, 3327 (2016).
- ¹⁷²G. McFiggans, D. O. Topping, and M. H. Barley, *Atmos. Chem. Phys.* **10**, 10255 (2010).
- ¹⁷³M. H. Barley, D. Topping, D. Lowe, S. Utembe, and G. McFiggans, *Atmos. Chem. Phys.* **11**, 13145 (2011).
- ¹⁷⁴D. O. Topping, M. H. Barley, and G. McFiggans, *Atmos. Chem. Phys.* **11**, 7767 (2011).
- ¹⁷⁵U. K. Krieger, F. Siegrist, C. Marcolli, E. U. Emanuelsson, F. M. Gøbel, M. Bilde, A. Marsh, J. P. Reid, A. J. Huisman, I. Riipinen, N. Hyttinen, N. Mlyly, T. Kurtén, T. Bannan, and D. Topping, "A reference data set for validating vapor pressure measurement techniques: Homologous series of polyethylene glycols," *Atmos. Meas. Tech.* (to be published).
- ¹⁷⁶H. Stark, R. L. N. Yatawelli, S. L. Thompson, H. Kang, J. E. Krechmer, J. R. Kimmel, B. B. Palm, W. Hu, P. L. Hayes, D. A. Day, P. Campuzano-Jost, M. R. Canagaratna, J. T. Jayne, D. R. Worsnop, and J. L. Jimenez, *Environ. Sci. Technol.* **51**, 8491 (2017).
- ¹⁷⁷Y. You, L. Renbaum-Wolff, M. Carreras-Sospedra, S. J. Hanna, N. Hiranuma, S. Kamal, M. L. Smith, X. Zhang, R. J. Weber, J. E. Shilling, D. Dabdub, S. T. Martin, and A. K. Bertram, *Proc. Natl. Acad. Sci. U. S. A.* **109**, 13188 (2012).
- ¹⁷⁸Y. You, M. L. Smith, M. J. Song, S. T. Martin, and A. K. Bertram, *Int. Rev. Phys. Chem.* **33**, 43 (2014).
- ¹⁷⁹L. Renbaum-Wolff, M. J. Song, C. Marcolli, Y. Zhang, P. F. F. Liu, J. W. Grayson, F. M. Geiger, S. T. Martin, and A. K. Bertram, *Atmos. Chem. Phys.* **16**, 7969 (2016).
- ¹⁸⁰E. S. Robinson, N. M. Donahue, A. T. Ahern, Q. Ye, and E. Lipsky, *Faraday Discuss.* **189**, 31 (2016).
- ¹⁸¹L. Mitchem, J. Buajareern, A. D. Ward, and J. P. Reid, *J. Phys. Chem. B* **110**, 13700 (2006).
- ¹⁸²J. P. Reid, B. J. Dennis-Smith, N.-O. A. Kwamena, R. E. H. Miles, K. L. Hanford, and C. J. Homer, *Phys. Chem. Chem. Phys.* **13**, 15559 (2011).
- ¹⁸³D. J. Stewart, C. Cai, J. Nayler, T. C. Preston, J. P. Reid, U. K. Krieger, C. Marcolli, and Y. H. Zhang, *J. Phys. Chem. A* **119**, 4177 (2015).
- ¹⁸⁴M. B. Altaf and M. A. Freedman, *J. Phys. Chem. Lett.* **8**, 3613 (2017).
- ¹⁸⁵J. Ovadnevaite, A. Zuend, A. Laaksonen, K. J. Sanchez, G. Roberts, D. Ceburnis, S. Decesari, M. Rinaldi, N. Hodas, M. C. Facchini, J. H. Seinfeld, and C. O'Dowd, *Nature* **546**, 637 (2017).
- ¹⁸⁶R. E. H. Miles, K. J. Knox, J. P. Reid, A. M. C. Laurain, and L. Mitchem, *Phys. Rev. Lett.* **105**, 116101 (2010).
- ¹⁸⁷A. E. Haddrell, J. F. Davies, and J. P. Reid, *Environ. Sci. Technol.* **49**, 14512 (2015).
- ¹⁸⁸D. L. Bones, J. P. Reid, D. M. Lienhard, and U. K. Krieger, *Proc. Natl. Acad. Sci. U. S. A.* **109**, 11613 (2012).
- ¹⁸⁹Y. C. Song, A. E. Haddrell, B. R. Bzdek, J. P. Reid, T. Bannan, D. O. Topping, C. Percival, and C. Cai, *J. Phys. Chem. A* **120**, 8123 (2016).
- ¹⁹⁰C. S. Handscomb, M. Kraft, and A. E. Bayly, *Chem. Eng. Sci.* **64**, 628 (2009).
- ¹⁹¹A. B. D. Nandiyanto and K. Okuyama, *Adv. Powder Technol.* **22**, 1 (2011).
- ¹⁹²A. Baldelli and R. Vehring, *Aerosol Sci. Technol.* **50**, 1130 (2016).
- ¹⁹³D. M. Lienhard, A. J. Huisman, U. K. Krieger, Y. Rudich, C. Marcolli, B. P. Luo, D. L. Bones, J. P. Reid, A. T. Lambe, M. R. Canagaratna, P. Davidovits, T. B. Onasch, D. R. Worsnop, S. S. Steimer, T. Koop, and T. Peter, *Atmos. Chem. Phys.* **15**, 13599 (2015).
- ¹⁹⁴H. C. Price, J. Mattsson, Y. Zhang, A. K. Bertram, J. F. Davies, J. W. Grayson, S. T. Martin, D. O'Sullivan, J. P. Reid, A. M. J. Rickards, and B. J. Murray, *Chem. Sci.* **6**, 4876 (2015).
- ¹⁹⁵R. M. Bain, C. J. Pulliam, and R. G. Cooks, *Chem. Sci.* **6**, 397 (2015).
- ¹⁹⁶S. Banerjee, E. Gnanamani, X. Yan, and R. N. Zare, *Analyst* **142**, 1399 (2017).
- ¹⁹⁷D. O. De Haan, L. N. Hawkins, J. A. Kononenko, J. J. Turley, A. L. Corrigan, M. A. Tolbert, and J. L. Jimenez, *Environ. Sci. Technol.* **45**, 984 (2011).
- ¹⁹⁸A. Fallah-Araghi, K. Meguellati, J. C. Baret, A. El Harrak, T. Mangeat, M. Karplus, S. Ladame, C. M. Marques, and A. D. Griffiths, *Phys. Rev. Lett.* **112**, 028301 (2014).
- ¹⁹⁹J. K. Lee, S. Kim, H. G. Nam, and R. N. Zare, *Proc. Natl. Acad. Sci. U. S. A.* **112**, 3898 (2015).
- ²⁰⁰R. M. Bain, C. J. Pulliam, F. Thery, and R. G. Cooks, *Angew. Chem., Int. Ed.* **55**, 10478 (2016).
- ²⁰¹A. K. Y. Lee, R. Zhao, R. Li, J. Liggio, S. M. Li, and J. P. D. Abbatt, *Environ. Sci. Technol.* **47**, 12819 (2013).
- ²⁰²R. J. Weber, H. Y. Guo, A. G. Russell, and A. Nenes, *Nat. Geosci.* **9**, 282 (2016).
- ²⁰³J. D. Surratt, M. Lewandowski, J. H. Offenberg, M. Jaoui, T. E. Kleindienst, E. O. Edney, and J. H. Seinfeld, *Environ. Sci. Technol.* **41**, 5363 (2007).
- ²⁰⁴D. J. Losey, R. G. Parker, and M. A. Freedman, *J. Phys. Chem. Lett.* **7**, 3861 (2016).

- ²⁰⁵T. Fang, H. Y. Guo, L. H. Zeng, V. Verma, A. Nenes, and R. J. Weber, *Environ. Sci. Technol.* **51**, 2611 (2017).
- ²⁰⁶C. J. Hennigan, J. Izumi, A. P. Sullivan, R. J. Weber, and A. Nenes, *Atmos. Chem. Phys.* **15**, 2775 (2015).
- ²⁰⁷D. C. Crans and N. E. Levinger, *Acc. Chem. Res.* **45**, 1637 (2012).
- ²⁰⁸J. D. Rindelaub, R. L. Craig, L. Nandy, A. L. Bondy, C. S. Dutcher, P. B. Shepson, and A. P. Ault, *J. Phys. Chem. A* **120**, 911 (2016).
- ²⁰⁹R. L. Craig, L. Nandy, J. L. Axson, C. S. Dutcher, and A. P. Ault, *J. Phys. Chem. A* **121**, 5690 (2017).
- ²¹⁰E. C. Griffith, B. K. Carpenter, R. K. Shoemaker, and V. Vaida, *Proc. Natl. Acad. Sci. U. S. A.* **110**, 11714 (2013).
- ²¹¹S. Rossignol, L. Tinel, A. Bianco, M. Passananti, M. Brigante, D. J. Donaldson, and C. George, *Science* **353**, 699 (2016).
- ²¹²J. W. Cremer, K. M. Thaler, C. Haisch, and R. Signorell, *Nat. Commun.* **7**, 10941 (2016).
- ²¹³D. T. Liu, J. Whitehead, M. R. Alfarra, E. Reyes-Villegas, D. V. Spracklen, C. L. Reddington, S. F. Kong, P. I. Williams, Y. C. Ting, S. Haslett, J. W. Taylor, M. J. Flynn, W. T. Morgan, G. McFiggans, H. Coe, and J. D. Allan, *Nat. Geosci.* **10**, 184 (2017).
- ²¹⁴E. Amstad, F. Spaepen, and D. A. Weitz, *J. Phys. Chem. B* **120**, 9161 (2016).
- ²¹⁵A. Baldelli, M. A. Boraey, D. S. Nobes, and R. Vehring, *Mol. Pharm.* **12**, 2562 (2015).
- ²¹⁶A. E. Haddrell and R. J. Thomas, *Appl. Environ. Microbiol.* **83**, e00809-17 (2017).
- ²¹⁷A. D. Estillore, J. V. Trueblood, and V. H. Grassian, *Chem. Sci.* **7**, 6604 (2016).